Histol Histopathol (2003) 18: 943-968

http://www.hh.um.es

Histology and Histopathology

Cellular and Molecular Biology

Review

RNA is closely associated with human mast cell lipid bodies

A.M. Dvorak[1], E.S. Morgan[1] and P.F. Weller[2]

Departments of [1]Pathology and Medicine, Beth Israel Deaconess Medical Center and Harvard Medical School, Boston, USA

Summary. Both novel and multiple ultrastructural studies based on different principles show relationships of cytoplasmic lipid bodies and ribonucleic acid (RNA) of potential importance to RNA metabolism in human mast cells. The methods include general ultrastructural morphological observations, imaging of RNA with an EDTA regressive stain, imaging of the incorporation of radio labeled uridine by ultrastructural autoradiography, postembedding immunogold labeling of uridine, ribosomes and small nuclear ribonuclear proteins and ultrastructural in situ hybridization detection of poly(A)-positive messenger RNA. Altogether these studies implicate human mast cell lipid bodies in RNA metabolism and are analogous to earlier similar studies which showed that human mast cell granules also curtain RNA.

Key words: RNA, Lipid bodies, Mast cells, Ultrastructure

Introduction

Ribosomes were described initially as a small particulate component of the cytoplasm with a particular affinity for the outside surface of the endoplasmic reticulum (Palade and Porter, 1954; Palade, 1955). They were also noted attached to the cytoplasmic side of nuclear membranes and free in the cytoplasm. In an extensive survey, all cells were found to have these particles, but their frequency was increased in embryonic cells and glandular secretory cells (Palade, 1955). These morphological findings provided a basis for their isolation and the biochemical determination of their ribonucleoprotein (RNP) content (Palade and Siekevitz, 1956a,b). For years electron microscopists have noted focal ribosome collections in specific sites other than attached to endoplasmic reticulum. For example, fibrillogenesis in embryonic or functional muscle is distinguished by focal attachment of ribosomes to newly generated foci of thick and thin filaments (Dix and Eisenberg, 1990), and dendritic spines of nerves display free ribosomes near synaptic densities (Steward and Levy, 1982; Martone et al., 1996). The latter observations have led to the identification of specific mRNAs in similar areas of dendrites, synapses and in axons (Merlie and Sanes, 1985; Davis et al., 1987; Garner et al., 1988; Jirikowski et al., 1990, 1992). Other subcellular structures have been recorded as containing mRNA (Laitala-Leinonen et al., 1996; Barth et al., 1998), supporting the concepts of mRNA transport and site-specific localization as mechanisms for synthesizing specific proteins at their intended site of function (Gottlieb, 1990; Singer, 1993; Wilhelm and Vale, 1993; Rings et al., 1994; St Johnston, 1995; Hazelrigg, 1998; Oleynikov and Singer, 1998).

Mast cells are granule-packed classical secretory cells whose synthetic products include proteolytic enzymes, mediators of inflammation, proteoglycans and cytokines (Metcalfe et al., 1981; Schwartz and Austen, 1984; Gordon et al., 1990). Functionally, synthetic events precede and accompany product storage and secretion, and involve ribonucleic acid (RNA) metabolism. Professional secretory cells such as pancreatic acinar cells characteristically contain extensive ribosome-studded rows of rough endoplasmic reticulum (RER) with enclosed cisterns filled with protein-rich synthetic products (Palade, 1955). Mature human mast cells, in contrast, are relatively devoid of RER; free ribosomes are also a minor cytoplasmic component in unstimulated mature cells (Dvorak, 1989). Historically, electron microscopists have noted that, in human mast cells, electron-dense particles not unlike ribosomes could be seen closely associated with secretory granules, and that these granules were not always entirely encompassed by granule membranes (Kobayasi et al., 1968; Asboe-Hansen, 1971; Dvorak, 1989; Dvorak et al., 2000b).

That human mast cell secretory granules may be involved with RNA metabolism has recently been indicated by ultrastructural electron microscopic methods based on several different imaging properties

Offprint requests to: Dr. Ann M. Dvorak, Department of Pathology, East Campus, Beth Israel Deaconess Medical Center, 330 Brooklie Ave., Boston, MA 02215, USA. e-mail: advorak@caregroup.harvard.edu

(Dvorak et al., 2000b). In aggregate, these include the demonstration of granule-associated ribosomes with a modified Bernhard's EDTA regressive stain (Bernhard, 1969; Dvorak et al., 2000b; Dvorak and Morgan, 2001) ; localization of uridine to granules by ultrastructural autoradiography (Dvorak et al., 2000a,b) and by a postembedding immunogold method (Dvorak et al., 2000b; Dvorak and Morgan, 2000b); granule localization of poly(A) - positive mRNA stores with ultrastructural in situ hybridization (ISH) using a variety of general poly(U) probes (Dvorak et al., 2000b; Dvorak and Morgan, 2000a); and the immunogold detection of ribonucleoproteins known to associate with small nuclear RNAs involved in splicing of pre-mRNAs to produce mRNAs for subsequent protein synthesis, (Busch et al., 1982; Hinterberger et al., 1983; Reddy and Busch, 1983; Konarska and Sharp 1987; Maniatis and Reed, 1987; Reed et al., 1988; Lobo and Hernandez, 1989) in granules (Dvorak et al., 2000b; Dvorak and Morgan, 2000b), and with ribosomes (Elkon et al., 1985, 1986), the organelle responsible for protein synthesis.

During the experiments designed to establish a role for HMC granules in RNA biology we noted that another prominent cytoplasmic organelle, lipid bodies, also had close associations with ribosomes. These were even more difficult to discern, than those associated with granules, in routine preparations since HMC lipid bodies are characterized by intense osmiophila which often effectively obscures internal structures and structures associated with the phospholipid-rich shell encasing lipid bodies. Nevertheless, images consistent with lipid body-ribosome association were present.

Lipid bodies are cytoplasmic organelles which are present in virtually all mammalian cells (Galli et al., 1985; Zweytick et al., 2000; Brown, 2001; Murphy, 2001). They are morphologically distinctive, roughly spherical, and, although lacking a classical trialminar unit membrane investiture are contained by a variably thick and variably present electron dense surface single membrane or shell (Dvorak, 1991). Lipid bodies typically are enmeshed in cytoskeletal filaments (Franke et al., 1987; Dvorak, 1991) . Lipid bodies have also been described in plant cells and seeds (Brown, 2001; Murphy, 2001) and in microorganisms (Murphy, 2001). These enigmatic organelles have been variously referred to as lipid droplets, lipid particles, and oil bodies, as well as lipid bodies (Zweytick et al., 2000).

Our initial interest in HMC lipid bodies led to studies which indicate that these organelles have novel functions as specialized intracellular domains involved in the formation of eicosanoids by cells engaged in inflammation (Dvorak et al., 1983, 1984; Galli et al., 1985; Weller and Dvorak, 1985; Weller et al., 1989; Weller et al., 1991a-c; Bozza et al., 1997). These studies revealed that leukocyte lipid bodies contain stores of esterfied arachidonic acid and that specific enzymes pertinent to arachidonate mobilization and oxidative metabolism are contained within them. Thus, lipid bodies are distinct cytoplasmic organelles which are both non-membrane stores of arachidonic acid and intracellular loci active in the regulated metabolism of arachidonate (Weller et al., 1991a). Since these studies of arachidonate metabolism we have implicated HMC lipid bodies in cytokine biology using immunogold analyses that have localized TNF-alpha and bFGF to lipid bodies (Beil et al., 1995; Dvorak et al., 2001).

Are lipid bodies, like secretory granules in HMCs, also subcellular sites/organelles that are important in RNA biology? The studies reported herein serve to implicate these organelles in the RNA biology of HMCs using a multimodal, ultrastructural approach.

Materials and methods

Human mast cells

Cells used for this study were isolated from surgically removed human lungs, remote from diseased areas, partially purified or cultured, as in previous reports (Schulman et al., 1982; Dvorak et al., 1984, 1985, 1986, 1987, 1988b; Hammel et al., 1985). Other samples derived from biopsies of human lesions taken for diagnostic purposes (Dvorak, 1987).

Routine electron microscopy preparation

Cells were fixed in a dilute mixture of aldehydes, washed in sodium cacodylate buffer, and placed in an agar pellet for further processing for electron microscopy (Dvorak, 1987). Samples were post-fixed in osmium and stained *en bloc* in uranyl acetate prior to dehydration and embedding. This was accomplished by dehydration in a graded series of alcohols, infiltration and embedding in a propylene oxide-Epon sequence to produce hard blocks for diamond-knife sectioning and polymerization for 16 h at 60 °C. Thin sections were cut using a Reichert ultramicrotome (Leica, Deerfield, IL, USA) and mounted on uncoated copper 200-mesh grids before staining with lead citrate and viewing with an electron microscope.

Bernhard's regressive ethylene diamine tetracetic acid (EDTA) stain for RNA

The staining solutions were aqueous uranyl acetate (UA) and lead citrate (LC), the latter prepared according to Reynolds (Reynolds, 1963). Staining in uranyl acetate was varied over 1-15 min and was done at room temperature and at 40 °C. Staining with lead citrate was done at 1, 5 or 10 min at room temperature. The chelating agent used was 0.2 M EDTA, 30 min at room temperature, 37 °C or 50 °C. The staining sequence was UA→EDTA→LC. In multiple evaluations, it was determined that the optimal staining conditions and sequence for our material was 15 min in 3% aqueous UA at 40 °C, 30 min in 0.2 M aqueous EDTA disodium salt at room temperature, and 1 min in LC at room temperature. This staining procedure varies somewhat

from the original procedure reported by Bernhard (Bernhard, 1969), where the UA concentration was 5% or 0.5% for 1 min, the EDTA concentration was 0.2 M for 30 min to 1 h, and the LC staining was 5 sec to 1 min, all done at room temperature on glutaraldehyde-fixed tissues embedded in Epon or glycol methacrylate.

RNase-gold, an enzyme affinity gold ultrastructural method to image RNA

As reported (Bendayan, 1981) section-containing grids were inverted and floated section side down on a phosphate-buffered saline (PBS) drop for 5 min followed by incubation on a drop of ribonuclease (RNase)-gold for 1 hr at 37 °C, pH 7.5. The grids were washed sequentially in PBS and distilled water and stained with lead citrate for 3-10 min before examination with an electron microscope.

Specificity controls as described (Bendayan, 1981), and additional controls were done to determine the nature of human mast cell (HMC) labeling with RNase-gold as follows. Samples were stained with the uncomplexed colloidal gold suspension alone, with an irrelevant protein-gold complex (bovine serum albumin (BSA)-gold), with an irrelevant enzyme-gold complex (deoxyribonuclease (DNase)-gold), or with an RNase-gold complex whose enzyme activity was destroyed by heating at 100 °C for 10 min. The effect of temperature, pH, and time on HMC granule staining with RNase-gold was examined by staining at 4 °C, 20 °C, and 37 °C, by staining at variable pHs from 4.5 to 8.7, and by staining for 5 or 60 min. Agar blocks containing macromolecules, RNA 16 mg/ml, heparin 20-30 mg/ml, polyuridine (U) 10 mg/ml, polyadenine (A) 20 mg/ml, chondroitin sulfate (CS) 26 mg/ml, or histamine 53 mg/ml, were fixed and processed similarly to the schedule for tissue blocks or cell suspensions and were stained with enzyme-gold complexes or gold suspension alone. Tissue and cell samples were also stained *en grid* with RNase-gold previously absorbed with heparin-agarose beads or Sepharose beads, with or without additional exposure of the RNase-gold to RNA or heparin (1 mg/ml) in solution (Dvorak and Morgan, 1998).

Ultrastructural autoradiographic imaging of RNA

Established methods (Caro et al., 1962; Bachmann and Salpeter, 1965; Kopriwa, 1973, 1975; Dvorak et al., 1983, 1984; Kopriwa et al., 1984) for the preparation of ultrastructural autoradiography samples of human mast cells exposed to [^{3}H]-uridine prior to fixation were used. A wire loop was used to place a thin film of liquid Ilford L4 photographic emulsion (Polysciences, Worthington, PA, USA) over thin sections on copper girds. Specimens were then exposed at 4 °C for varying times, developed either in Microdol-X (Kodak, Rochester, NY, USA) or in physical developer followed by gold latensification (Kopriwa, 1973, 1975; Kopriwa et al., 1984), and stained in lead citrate. Freshly prepared physical developer solution contained 0.75 g of Elon (Kodak), 0.5 g of sodium sulfite, 0.2 g of potassium thiocyanate in 100 ml of distilled water (H_2O), and gold thiocyanate contained 0.5 ml of 2% gold tetrachloride, 0.125 g of potassium thiocyanate, 0.15 g of potassium bromide in 250 ml of distilled water. The development sequence used was as follows: (1) 1 min in distilled H_2O; (2) 1 min in gold thiocyanate; (3) rinse in H_2O; (4) 6 min in physical developer solution, and (5) H_2O rinse.

Ultrastructural immunogold cytochemistry with an antibody to uridine

A standard postembedding immunogold protocol (Dvorak et al., 1988a) was used. The primary antibody was a rabbit polyclonal anti-uridine (Research Plus, Bayonne, NJ) that is stable with formaldehyde fixation (manufacturer's literature) (Dvorak and Morgan, 2000b). Secondary antibodies were either a goat anti-rabbit 20 nm gold (EY Laboratories, San Mateo, CA) or a goat anti-rabbit 5 nm gold (Amersham Pharmacia Biotech, Piscataway, NJ).

The general steps for this protocol include the following: unmask, permeabilize, block, primary antibody, wash, secondary gold-labeled antibody, wash, stain. Multiple variations of these steps were done. For unmasking, we evaluated sodium metaperiodate (Dvorak et al., 1988a), hydrogen peroxide (Dvorak et al., 1988a), and hyaluronidase (Qu et al., 1998a,b), at variable times and concentrations. The permeabilizing step(s) was done by adding 0.1% Triton-X to the wash steps, and blocking was done with normal goat serum (NGS) and bovine serum albumin (BSA). Grids containing sections were ultimately stained with uranyl acetate and lead citrate or with lead citrate alone.

Ultrastructural cytochemical, immunocytochemical and *in situ* hybridization methods with polyuridine probes

Adaptations for electron microscopy of standard methods of in situ hybridization (ISH) were used (Lamb and Laird, 1976; Capco and Jeffery 1978; Binder et al., 1986; Dvorak and Morgan 2000a). Use of variously labeled poly(U) probes allowed imaging of poly(A) positive mRNA in subcellular organelles and locations (Dvorak and Morgan, 2000a). Preparation of these probes, various direct binding and ISH protocols, and reporters for viewing them are detailed next.

Ultrastructural ISH using [^{3}H]-polyuridine

The method reported by Capco and Jeffery (Capco and Jeffery, 1978) for light microscopy was followed exactly, as well as with some modifications for ultrastructural imaging. Specific steps included the following *en grid* treatments: (1) rinse for 5 min in 0.1 M Tris-HCl buffer, 20 °C (or 37 °C), containing 0.003 M

$MgCl_2$, pH 7.6; (2) digest for 1 h, 37 °C, in same buffer with 100 mg/ml DNase I (EC 3.1.21.1, Sigma, St. Louis, MO); (3) repeat step 1; (4) rinse for 5 min, 20 °C (or 50 °C), in 0.01 M Tris-HCl buffer containing 0.005 M MgCl2 and 0.2 M NaCl, pH 7.6; (5) anneal in a sealed chamber for 16 h, 50 °C, with 0.9 mCi [^{3}H]-polyU/ml (New England Nuclear, Boston, MA; specific activity: 3.37 Ci/mmol, UMP, Lot 2284-274, Polyuridylic acid, sodium salt, [5,6-[3H]-uridylate]) in the same buffer; (6) repeat step 4; (7) rinse for 5 min, 20 °C (or 37 °C), in 0.05 M Tris buffer containing 0.001 M MgCl2 and 0.1 M KCl, pH 7.6; (8) digest for 1 h, 37 °C, in 1 mg/ml RNase (EC 3.1.27.5, bovine pancreas; Sigma, St. Louis, MO) in 0.05 M Tris-HCl buffer containing 0.001 M $MgCl_2$ and 0.1 M KCl, pH 7.6; (9) repeat step 7; (10) rinse x 2 in distilled water, 20 °C; (11) rinse for 15 min, 4 °C, in 2% trichloroacetic acid (TCA) (Sigma, St. Louis, MO); (12) repeat step 10; (13) air dry; (14) cover section on the grid with a loop of Ilford 4 photographic emulsion (Polysciences, Warrington, PA) as described (Dvorak et al., 1984); (15) expose at 4 °C for 7 and 21 days; (16) develop with Microdol X (Kodak, Rochester, NY), as described previously (Dvorak et al., 1984) or with physical solution for small grains as described by (Kopriwa, 1973); (17) stain with 0.25% lead citrate, 3 min. Controls included omission of either the DNase digestion or RNase digestion steps.

Variations in the sequence for ISH using [^{3}H]-polyU included doubling the 5-min single buffer rinses, omission of the TCA step, and digesting the photographic emulsion with 1 mg/ml proteinase K (EC 3.4.21.64, Sigma, St. Louis, MO), 30 min, 37 °C or with 0.5% or 1% subtilisin A (EC 3.4.21.14; Boehringer Mannheim Biochemical, Indianapolis, IN) 15 min, 40 °C during Microdol-X development and before staining the grids with lead citrate and/or uranyl acetate.

Ultrastructural ISH using polyuridine-gold

A colloidal gold suspension was prepared according to principles reported by Frens (Frens, 1973). Briefly, 4 ml of an aqueous 1% solution of sodium citrate (Sigma, St. Louis, MO) was added to a boiling aqueous solution of 100 ml 0.01% tetrachloroauric acid (Sigma, St. Louis, MO) and allowed to boil for 5 min before cooling on ice. The pH of the colloidal gold suspension so produced was adjusted to 7.4 with 0.2 M potassium carbonate, K_3Co_3. Preparation of the poly(U)-gold complex was according to the method of Bendayan (Bendayan, 1981). Specifically, 0.7 mg of the lyophilized potassium salt of polyuridylic acid (LKB, Pharmacia, Piscataway, NJ) was dissolved in 1 ml distilled water and placed in a polycarbonate ultrafuge tube with 10 ml of the gold suspension. The mixture was centrifuged at 25,000 rpm for 30 min, at 4 °C, in a Beckman ultracentrifuge with a 50.2 Ti rotor. The poly(U)-gold complex formed a red sediment that was carefully recovered and resuspended in 3 ml 0.1 M phosphate-buffered saline (PBS) containing 0.02% polyethylene glycol (JT Baker, Phillipsburg, NJ), pH 7.6 (final concentration 0.25 mg poly[U]/ml). Initially, the poly(U)-gold reagent was used for direct staining of sections on grids, as reported for other gold conjugates (Bendayan, 1981); section-containing grids were inverted and floated on PBS drops for 5 min, followed by incubation on a drop of poly(U)-gold at 37 °C for 60 min. The grids were vigorously washed in distilled water and stained with dilute lead citrate for 10 min before viewing in a Philips 300 or 400 microscope. Additionally, preparation of poly(U)-gold, as in the report for the preparation of polyadenine (poly[A]-gold (Dworetzky and Feldherr, 1988)), was done. This method included placing 0.5 mg poly(U) in 1 ml of a phosphate buffer containing 7.2 mM K_2PO_4, 4.8 mM KH_2PO_5, 10 mM KCl at pH 7.0 prior to mixing with sodium citrate-reduced tetrachloroauric acid colloidal gold solution. After centrifugation, the poly(U)-gold reagent was resuspended in 3 ml of PBS containing 0.02% polyethylene glycol and used for direct staining of sections en grid, as above. The in situ hybridization sequence for light microscopy, reported by Capco and Jeffery (1978) and adapted for electron microscopy, was followed (see earlier), except that annealing was done in a sealed chamber for 16 h at 50 °C with PBS containing poly(U)-gold. Controls for the direct en grid staining with poly(U)-gold or for the ISH protocol using poly(U)-gold were done. These included absorption of the poly(U)-gold reagent with poly(U) or poly(A) beads (LKB, Pharmacia, Piscataway, NJ) prior to proceeding with either direct or ISH protocols with the absorbed reagent. Similarly, use of the stabilized gold solution alone or after absorption with poly(U) beads or poly(A) beads was done in either protocol.

The specificity of the poly(U)-gold reagent for these protocols was further evaluated by staining sections of agar (Bactoagar, Difco Labs, Detroit, MI) blocks containing either poly(U) (20 mg/ml) or poly(A) (20 mg/ml) that were processed as the mast cell suspensions were for electron microscopy.

Ultrastructural ISH using biotinylated polyuridine

Poly(U) (polyuridylic acid, lyophilized potassium salt [LKB Pharmacia, Piscataway, NJ]) was photobiotinylated using Photoprobe (long arm) biotin (Vector Labs, Burlingame, CA), as reported (Forster et al., 1985; McInnes et al., 1987). Briefly, 0.5 mg of the photoprobe-biotin was reconstituted at 0.5 ml 0.1 mM EDTA, pH 8.0. Fifty microlitres (50 ml) of this stock solution was used to prepare a photoprobe-biotin, poly(U) solution by combining it with 50 ml of a 1 mg/ml poly(U) solution previously made with 0.1 mM EDTA, pH 8.0. The combined solutions were placed in a microfuge tube and irradiated on ice with a sunlamp (Vector Labs, Burlingame, CA) shining directly into the microfuge tube opening for 15 min at a distance of 10 cm. Recovery of the photobiotinylated poly(U) was as follows. The volume of irradiated reagent was increased with 100 ml 0.1 M Tris-HCl, pH 9.0, and 100 μl 2-

butanol (Sigma, St. Louis, MO) and centrifuged for 2 min at 12,000 rpm in a Beckman microfuge (Palo Alto, CA). After discarding the upper phase, a repeat extraction in 100 μl 2-butanol was carried out. Then, 10 mg of ribonucleic acid (RNA; Worthington, Freehold, NJ) was added and nucleic acid was precipitated with 0.75 ml 4 M NaCl and 0.125 μl ethanol. After cooling at -20°C overnight and centrifugation, the reagent was speed-vacuumed to dryness. The biotinylated polyuridine was dissolved in 0.1 mM EDTA, pH 8.0, for use in ISH protocols.

Two ISH protocols with modifications (Capco and Jeffery, 1978; Binder et al., 1986) were used to localize mRNA in human mast cells with the biotinylated poly(U) probe (Langer et al., 1981; Singer and Ward, 1982). A modification for electron microscopy of a light microscopy protocol (Capco and Jeffery, 1978) (see earlier) was performed. Initially, grids were digested with proteinase K (0.125 or 0.25 mg/ml in PBS) at 30 °C, or 60 min at 20 °C, and the ISH protocol followed thereafter. Annealing in a sealed chamber was done for 16 h at 50 °C with the biotinylated poly(U) probe in 0.1 mM EDTA, pH 8.

In another protocol for electron microscopic ISH (Binder et al., 1986), annealing was done in a moist chamber for 24 h with biotinylated poly(U) in 0.1 mM EDTA, pH 8, at 37 °C. Several reporter methods were used to image mRNA after ISH with the poly(U)-bound Photoprobe (long arm) biotin. These include an immunogold protocol as follows: (1) wash x 3, 10 min each, in 0.1 M Tris-buffered saline (TBS) PH 7.6 containing 0.1% bovine serum albumin (BSA); (2) block for 20 min with TBS-BSA and 5% normal rabbit serum (NRS) (Sigma, St. Louis, MO); (3) incubation in primary antibody, affinity-purified goat antibiotin (Vector Labs, Burlingame, CA), 1:1 dilution in 0.1 M TBS-BSA plus 1% NRS and 0.1% Tween-20 for 1 h at 20°C; (4) wash x 3, 10 min each, in TBS-BSA; (5) incubate with secondary antibody (20 nm-labeled rabbit anti-goat, EY Labs, San Mateo, CA), 1:20 dilution in TBS-BSA with 1% NRS, 0.1% Tween-20; (6) wash twice, 10 min each, in TBS-BSA; (7) wash twice, 10 min each, in distilled water; (8) dry overnight; (9) stain with 0.25% lead citrate, 5 min.

A second reporter method used protein A (Binder et al., 1986), as follows: (1) rinse five times, 10 min each, with 0.1 M Tris-HCl-buffered saline (TBS) with 0.1% BSA (TBS-BSA); (2) incubate for 2 h at 20 °C in goat antibiotin antibody (Vector Labs, Burlingame, CA), diluted 1:50 in 0.1 M TBS-BSA with 1% fish gel (Sigma, St. Louis, MO) and 0.1% Tween-20 (Fisher Scientific, Fairlawn, NJ); (3) wash twice for 2 min each with TBS-BSA; (4) incubate for 1 h, 20 °C, with protein A-gold, 20 nm (Bendayan and Zollinger, 1983) (Probetech, Buckingham, PA), 1:5 dilution in 0.1 M TBS-BSA contain 1% fish gel and 0.1% Tween-20; (5) wash twice, 2 min each, in TBS-BSA; (6) wash in distilled water; (7) stain with 0.25% lead citrate, for 5 min.

A third reporter system used a streptavidin-gold protocol (Hiriyanna et al., 1988). In this method, after the incubation of goat-antibiotin antibody (Vector Labs, Burlingame, CA) diluted 1:50 as done earlier and 2 x washes for 2 min each with TBS-BSA, the grids were incubated in streptavidin-gold (10 nm) diluted 1:10 for 1 h, at 20 °C. Following this, two washes in TBS-BSA and then in distilled water preceded staining with 0.25% lead citrate for 5 min.

A fourth reporter system used goat antibiotin 10-nm gold (EY Labs, San Mateo, CA) to directly label biotinylated poly(U) after the electron microscopy ISH protocol.

Controls and variations in the protocols were carried out. In some cases, proteinase K digestion was omitted to evaluate the necessity for this step. In other cases, the concentration of proteinase K and digestion time were decreased. Another variation was to use hyaluronidase (EC 3.2.1.35; Sigma, St. Louis, MO) in either PBS or sodium acetate buffer, 2.5 mg/ml, 30 min, as a substitute for the proteinase K digestion. Some samples were examined without hybridization to determine the binding capacity of Photoprobe (long arm) biotin-labeled poly(U) directly to the electron microscopy samples. Controls included omission of the biotinylated poly(U) probe only and omission of the probe, together with the primary antibody to biotin, to determine whether the probe and antibody were essential for imaging with the gold-labeled secondary antibody (and, thus, specific for poly(A) in mRNA and for biotin in the biotinylated poly(U) probe, respectively).

Controls for the protein A-gold reporter were as follows: omission of the hybridization step to determine binding of biotinylated poly(U) directly to the sample, omission of the antibiotin antibody to determine non-specific sticking of protein A-gold to the biotinylated poly(U) probe, omission of biotinylated poly(U) to determine non-specific binding of the antibiotin antibody to the sample, and omission of biotinylated poly(U) and the antibiotin antibody to determine non-specific sticking of protein A-gold to the sample.

Specificity controls for streptavidin-gold and goat-antibiotin-gold included omission of the biotinylated poly(U) probe for either reporter.

Ultrastructural ISH using BSA-conjugated polyuridine-gold

The BSA-poly (U)-gold reagent was prepared according to principles reported for glutaraldehyde-assisted conjugation (Avrameas, 1969; Geoghegan and Ackerman, 1977; Horisberger and Rosset, 1977; Brooks and Binnington, 1989). BSA was first conjugated to poly(U) and then attached to colloidal gold (Frens, 1973), as reported for proteins and enzymes (Bendayan, 1981, 1989). Briefly, poly(U) (1 mg) and BSA (4 mg) were dissolved in 0.25ml of 0.005 M NaCl, adjusted to pH 7 with 0.1 M potassium carbonate (K2CO3). Glutaraldehyde, 0.05 ml, 0.25% (Electron Microscopy

Services, Fort Washington, PA) was added for 2 h at 25 °C, following which 12.2 ml of 0.005 M NaCl, pH 7, was added. The solution was filtered through a 0.45 mM Millipore filter (Millipore, Bedford, MA). A colloidal gold suspension (Frens, 1973) was prepared (see earlier): 0.3 ml of the filtered BSA-poly(U) solution and 10 ml of the colloidal gold were mixed manually for 2 min; 0.5 ml of filtered 1% polyethylene glycol 20 (Sigma, St. Louis, MO) was added to the mixture prior to centrifugation for 45 min at 35,000 rpm in an L8-80 Beckman centrifuge with a 50.2 Ti rotor. The BSA-poly(U)-gold reagent was resuspended in 4 ml of 0.05 M Tris-HCl buffer containing 0.15 M NaCl, 0.5 mg/ml polyethylene glycol and 0.5 mg/ml sodium azide, as previously reported for preparing protein-gold conjugates (Bendayan, 1981). The BSA-poly(U)-gold probe was stored at 4 °C and remained active for several months. After washing for 10 min in PBS containing 1 mM $MgCl_2$ and 1 mM $CaCl_2$, samples were stained en grid directly for 60 min in BSA-poly(U)-gold diluted 1:1 in the same buffer, rinsed in this buffer, followed by distilled water, and stained with lead citrate for 5 min. Other samples were stained with Tris-HCl substituted for PBS, or were used in several ISH protocols (Lamb and Laird, 1976; Capco and Jeffery, 1978; Binder et al., 1986), modified as follows.

One protocol for ISH was a long procedure originally described for light microscopy (Capco and Jeffery, 1978), which we modified for electron microscopic ISH (see earlier) (Dvorak and Morgan, 2000a). Annealing was done in a sealed chamber for 16 h, 50 °C, with 0.1 ml of the Tris-buffered BSA-poly (U)-gold probe.

Another protocol (Binder et al., 1986) for electron microscopic ISH was used (see earlier). In this protocol, the sample was annealed in a moist chamber for 24 h at 37 °C, in 0.05 M Tris-HCl buffer, pH 7.2, containing 0.15 M NaCl, 0.5 mg/ml polyethylene glycol and 0.1 ml of the Tris-buffered BSA-poly(U)-gold probe.

In order to decrease the lengthy ISH schedules, hoping for better preservation of substructural organelles such as lipid bodies, a shorter ISH schedule was adapted for use with the BSA-poly(U)-gold probe (Lamb and Laird, 1976). Briefly, 20 μl of the BSA-poly(U)-gold probe in 2xSSC (0.3 M sodium chloride and 0.03 M trisodium citrate) was annealed in a moist chamber to the samples for 3.5 h at 37 °C. Following this, samples were rinsed in cold 2xSSC and digested with 2 mg/ml pancreatic RNase in 2xSSC (EC 3.1.27.5; Sigma, St. Louis, MO), 20 min, 4 °C. Several rinses followed in cold 2xSSC over 2 h and grids were then stained for 5 min with 0.25% lead citrate.

Controls for these procedures included comparisons of the efficacy of various buffers (e.g., PBS, SSC, Tris-HCl), omission of the ISH step to evaluate direct binding of the probe, omission of RNase digestion, use of BSA alone coupled to gold in the ISH step, and the same with omission of the ISH step to detect binding not related to poly(U). In this case, the BSA was treated exactly as it was in the glutaraldehyde cross-linking procedure to poly(U) (e.g., 0.25% glutaraldehyde for 2 h, 25°C). The colloidal gold solution alone was also used to test for non-specific binding. This was done in buffers used for ISH and in conjunction with the ISH procedure.

Ultrastructural ISH with polyuridine, detected with an antibody to uridine and a postembedding immunogold procedure

We used a rabbit polyclonal antibody to uridine and a postembedding immunogold procedure to detect poly(U) bound to poly(A)-positive mRNA following ISH with an unlabeled poly(U) probe. Controls for the immunogold detection system included omission of the primary antibody, substitution with irrelevant IgG for the primary antibody, and absorption of the primary antibody with poly(A)- or poly(U)-sepharose before en grid staining as well as the controls for ISH (see earlier).

Ultrastructural immunogold cytochemistry with autoimmune human sera

Primary antibodies used for postembedding immunogold staining included the purified IgG fractions of screened and characterized human autoimmune disease plasma, containing anti-Sm, anti-RNP, anti-SS-A (Ro), anti-SS-B (La), anti-ribosomal P and anti-mitochondrial activity (all from ImmunoVision, Springdale, AZ). According to the manufacturer's specifications, the anti-Sm product showed a single Sm precipitation band when tested using double immunodiffusion against rabbit thymus extract and specificity was verified by identify of precipitation with Centers for Disease Control-Arthritis Foundation (CDC-AF) reference serum. In an ELISA system designed to detect all antibody classes, no reactivity with purified RNP, SS-B, or SS-A was present. The anti-RNP product showed a single precipitation RNP band when tested using double immunodiffusion against rabbit thymus extract, and specificity was verified by identity of precipitation with CDC-AF reference serum. In an ELISA system designed to detect all antibody classes, no reactivity occurred against purified Sm, SS-A, or SS-B. Similarly, verification studies for anti-SS-A against CDC-AF reference serum showed no reactivity with purified Sm, RNP or SS-B, and the product showed a single precipitation band for SS-A (Ro) in a double immunodiffusion against primate spleen extract; anti-SS-B, tested against CDC-AF reference serum, was not reactive against purified Sm or RNP, but a low level of anti-SS-A activity was present in an ELISA system that detects all antibody classes. This product showed only an SS-B precipitation band when tested by double immunodiffusion against rabbit thymus extract. The manufacturer's literature for human autoantibody against ribosomal P antigen states that this product showed a single precipitation band for ribosomal P when tested by immunodiffusion against rabbit thymus extract; no

reactivity against purified SS-A, SS-B, Sm, RNP and Jo-1 antigens was detected in an ELISA system designed to detect all IgG subclasses. Reference primary antibodies for SS-B, SS-A, Sm and RNP were also obtained from the Arthritis Foundation/Center for Disease Control (Atlanta, GA) and used for postembedding immunogold labeling.

Secondary antibodies labeled with gold particles included goat anti-human 15-nm-gold (GAH-15, Amersham Pharmacia Biotech, Piscataway, NJ), goat anti-human 20-nm gold (GAH-20, EY Laboratories, San Mateo, CA).

A standard postembedding immunogold protocol (Dvorak et al., 1988a) was used. The general steps for this protocol include the following: unmask, permeabilize, block, primary antibody, wash, secondary gold-labeled antibody, wash, stain. Multiple variations in these steps were done. For unmasking, we evaluated sodium metaperiodate (Sigma, St. Louis, MO) (Dvorak et al., 1988a), hydrogen peroxide (Fisher, Pittsburgh, PA) (Dvorak et al., 1988a), and hyaluronidase (EC 3.2.1.35, Sigma, St. Louis, MO) (Qu et al., 1998a,b), at variable times and concentrations. The permeabilizing step(s) was done by adding 0.1% Triton-X (Sigma, St. Louis, MO) to the wash steps, and blocking was done with normal goat serum (NGS) and bovine serum albumin (BSA) (Sigma, St. Louis, MO). Variable times and concentrations of primary antibodies were evaluated. Secondary antibody variations also included time and concentration differences as well as different gold sizes. Grids containing sections were ultimately stained with uranyl acetate and lead citrate or with lead citrate alone.

Controls included omission of the primary antibody to evaluate nonspecific sticking of the secondary antibody and replacement of the primary antibody with normal human serum (NHS), or with an irrelevant autoimmune human sera to mitochondria (ImmunoVision, Springdale, AZ).

Results

Ultrastructural anatomy of human mast cell lipid bodies suggest close relationships with ribosomes. Lipid bodies are variably osmiophilic, round structures of ~1-2 mm size that frequent the cytoplasm and perinuclear cytoplasmic areas of human mast cells (Dvorak, 1989) (Fig. 1). They are enmeshed in intermediate filaments (Fig. 1g) and often have cisterns of smooth endoplasmic reticulum molded to their curved surfaces (Fig. 1a,b). They are not invested with trilaminar unit membranes, but often show partial to complete investiture with an electron-dense shell of variable thickness. Because the electron density of lipid bodies often obscures peri- and intra-lipid body substructural details, little notice has been made of their possible ribosome interrelationships. We have noted three such possible relationships in routinely-prepared ultrastructural samples of human mast cells. These are 1.) clusters of free, cytoplasmic, electron dense ribosomes adjacent to lipid body surfaces (Fig. 1c,d,e) 2) linear arrays of ribosomes associated with lipid body surfaces (Fig. 1c) 3) focal, centrally located, electron lucent, rounded areas which contain electron dense ribosome-like particles within them, located in lipid bodies (Fig. 1f,g).

Close associations of ribosomes and lipid bodies in human mast cells demonstrated by staining with a chelating agent

We used a modification of Bernhard's method (Bernhard, 1969) to stain human mast cells. In this method, preferential bleaching of structures known to contain deoxyribonucleic acid (DNA) occurs with subsequent enhancement of the electron density of structures known to contain ribonucleic acid (RNA) (ribosomes). It is now generally conceded that the electron density so produced is based primarily on the protein moieties associated with RNA (Biggiogera et al., 1998; Biggiogera and Fakan, 1998). The EDTA regressive stain also bleaches the extreme electron density of mast cell granules (Dvorak and Morgan, 2001) and lipid bodies. This staining method provided a view of closely associated ribosomes with human mast cell lipid bodies in the cytoplasm and in the perinuclear location, adjacent to ribosome-filled nuclear pores (Fig. 2).

Ribonuclease-gold label RNA in human mast cell lipid bodies

We used an enzyme-affinity gold ultrastructural technique (Bendayan 1981, 1989; Dvorak and Morgan, 1998) designed to identify RNA-rich structures based on staining with an RNase-gold (R-G) probe in human mast cells (Fig. 3). Earlier, we determined that this method heavily labeled heparin, unique to mast cell granules, which was based on the specific binding of RNase, a known heparin inhibitor, to granule heparin (Dvorak and Morgan, 1998, 1999) (Fig. 3a). We were unable to quantitatively determine that this method also labeled granule RNA stores, although qualitative results suggested this possibility (Dvorak and Morgan, 1998). Lipid bodies, in the same samples of human mast cells, are not heparin-containing organelles; they avidly bound the R-G reagent indicating the presence of RNA in lipid bodies (Fig. 3a). Gold particles were present within lipid bodies, encircling them and bound to ribosome clusters nearby (Fig. 3b). When intralipid body electron lucent structures with electron dense particles were present, the R-G reagent also was bound to these structures (Fig. 3c). We used a variety of blocking and digestion protocols to evaluate heparin binding of the R-G reagent. We found that in all of these R-G staining of granules was diminished or absent (Fig. 3d), indicating the presence of heparin (Dvorak and Morgan, 1998, 1999), whereas lipid body staining did not change (Fig. 3b,c), indicating the presence of RNA in lipid bodies.

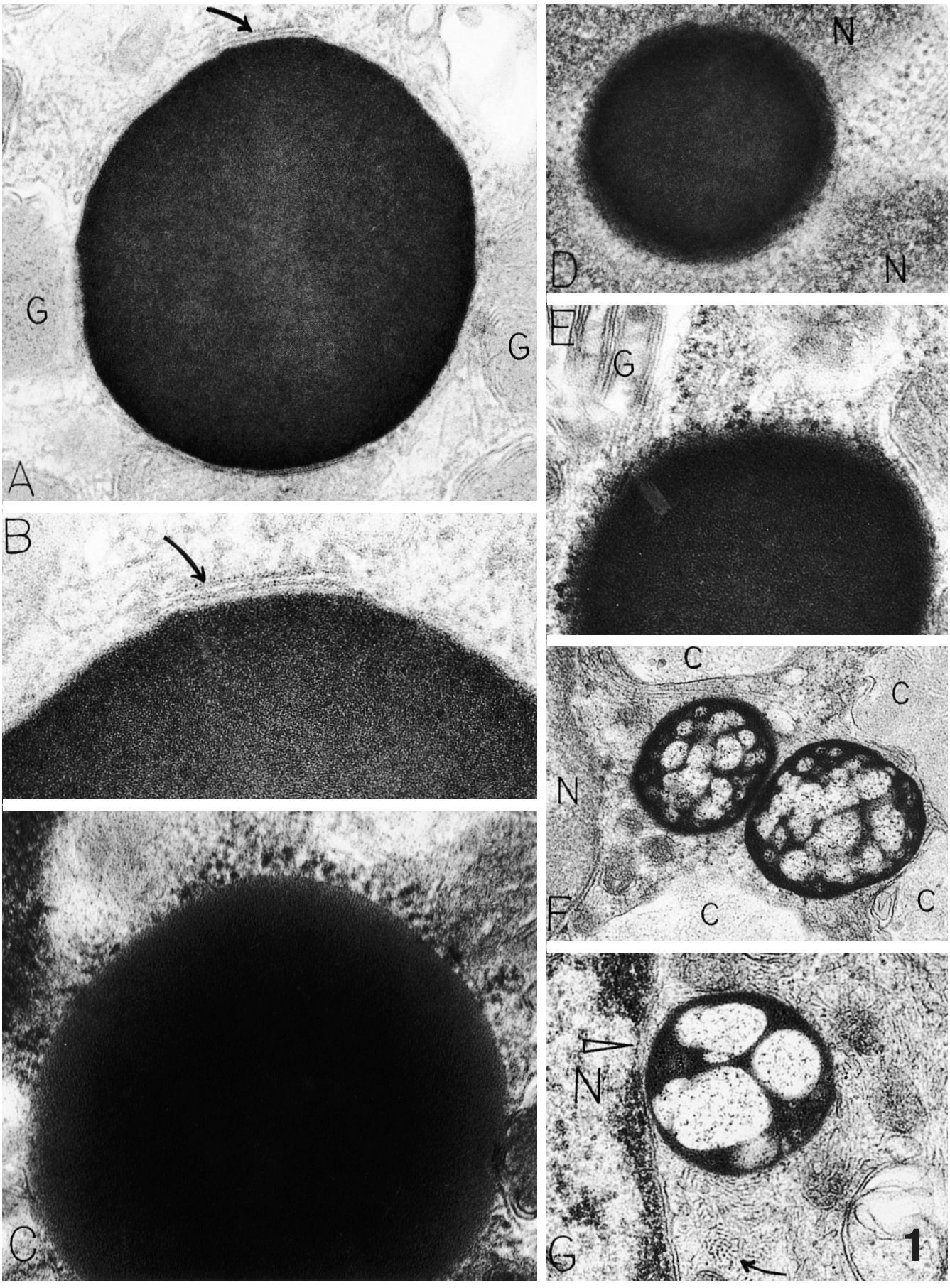
G
G
A
N
D
N
E
G
B
C
C
N
C
C
F
N
G
1

Fig. 1. Ultrastructural anatomy of HMC lipid bodies. **A-D**, 6 hr control cultures; **E**, 20 minute control; **F**, 20 minute degranulation; **G**, 6 hr recovery after degranulation culture. All panels are of routine osmium collidine uranyl en bloc (OCUB) prepared samples. The lipid bodies in all panels contain osmiophilic, electron dense material which appears to be homogeneous **(A-E)** or riddled with honeycombed vesicular structures within which electron dense particles are visible (**F, G**). LBs reside in the cytoplasm remote from the nucleus (**A-C, E)** and closely associated with nuclei **(D, F, G)**. Membrane-bound cisterns of smooth endoplasmic reticulum partially envelope lipid bodies (arrow, in **A**) seen at higher magnification in **B** (arrow). Clusters of free ribosomes are visible attached to lipid body surfaces **(C-E).** The LB in **G** is adjacent to a nuclear pore (arrowhead). Two lipid bodies are surrounded by degranulation channels **(C)** in the stimulated sample (**F**). The LB in **G** is enmeshed in intermediate filaments (arrow). G: granule; N : nucleus; C: channel; A, x 84,000; B, x 173, 500; C, x 85,000; D, x 70,000; E, x 79,000; F, x 41,000; G, x 60,000

Ultrastructural autoradiography of uridine incorporation labels RNA in human mast cell lipid bodies

Ultrastructural autoradiography of isotopically labeled uridine has been used for years to identify cellular RNA that has incorporated uridine (Fakan and Bernhard, 1971, 1973; Angelier et al., 1976; Fakan et al., 1976; Fakan and Puvion, 1980; Fakan, 1994). During extensive studies of such incorporation into control HMCs, that had degranulated, and HMCs undergoing recovery from degranulation (Dvorak et al., 2000a,b) we noted that, in addition to expected nuclear and cytoplasmic sites of RNA, cytoplasmic lipid bodies also incorporated [^{3}H]-uridine (Fig. 4). We noted the propensity for lipid bodies in close proximity to nuclear envelopes to incorporate [^{3}H]-uridine into RNA (Fig. 4) and that not all lipid bodies incorporated [^{3}H]-uridine. Secretory granules, a new finding (Dvorak et al., 2000a,b), also avidly incorporated this RNA precursor. Thus, the ultrastructural studies identified two new organellar sites of RNA—secretory granules (Dvorak et al., 200a,b) and lipid bodies.

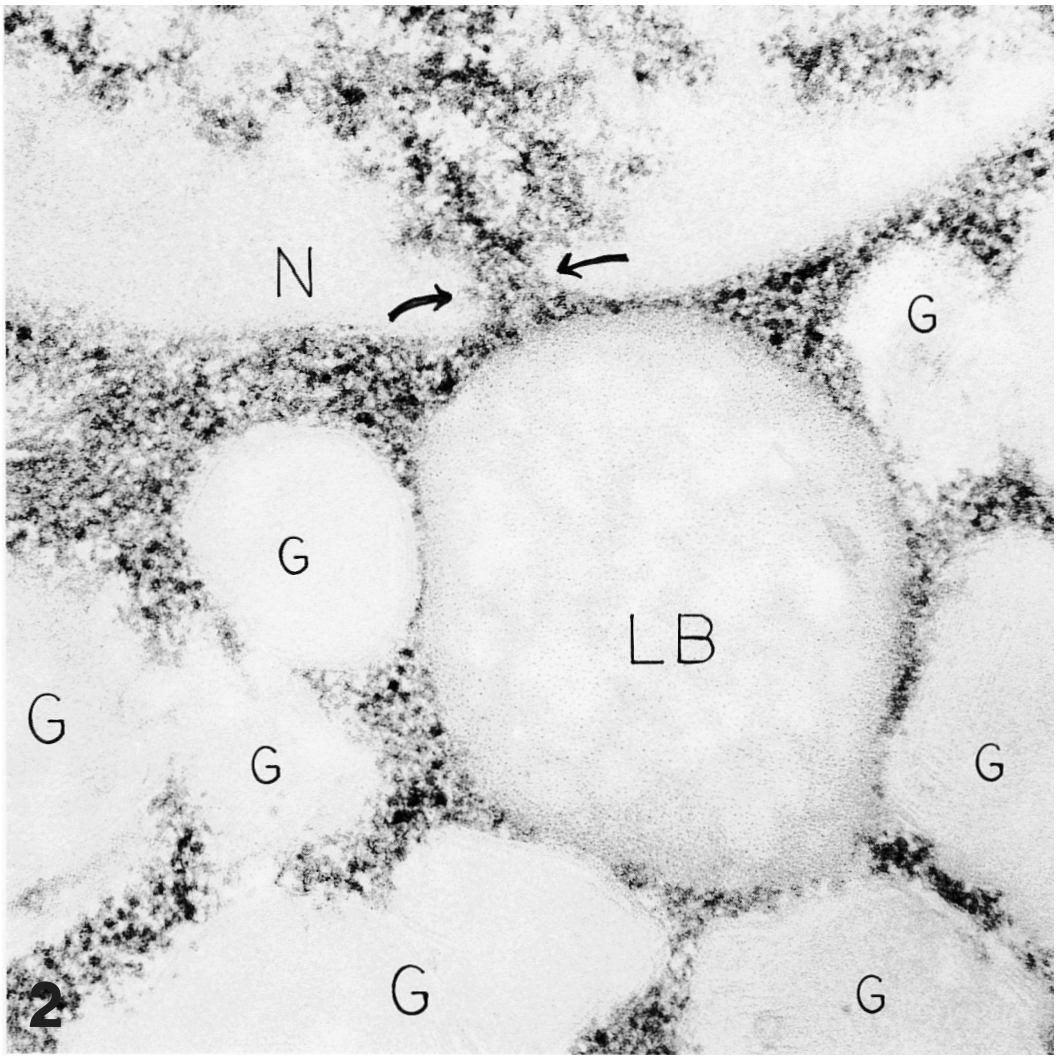

Fig. 2. HMC prepared with the EDTA regressive stain for RNA. Electron dense RNA and ribosomes fill the interchromatinic nuclear (N) matrix, the nuclear pore (arrows) and surround and attach to cytoplasmic granules (G) and a lipid body (LB). Nuclear chromatin, granule matrix and lipid body contents are bleached with this technique allowing better visualization of adjacent and attached electron dense ribosomes. N: nucleus; G: granule; LB: lipid body. x 74,000

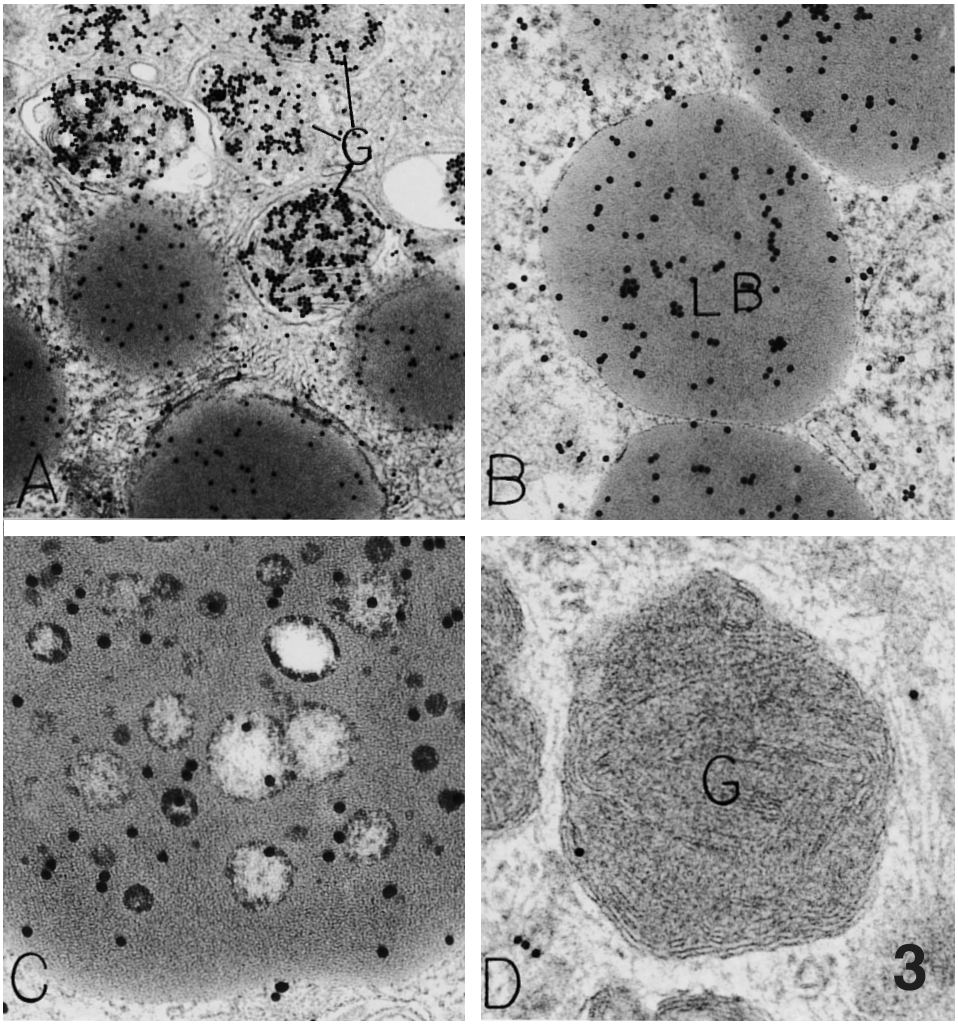

Fig. 3. Six hr control HMCs prepared with the enzyme affinity gold method to detect RNA using an RNase-gold probe. In **A**, RNase-gold binds to heparin in granules (G) and to RNA in adjacent lipid bodies. In **B**, absorption of the RNase-gold probe with heparin sepharose prior to sample staining did not abrogate binding to RNA in lipid bodies (LB) or to the numerous membrane attached and free ribosomes adjacent to LBs. In **C**, a similarly heparin-absorbed RNase-gold probe stains the RNA in the lipid body matrix and in the vesicular structures inside the LB matrix. Heparin absorption of the RNase-gold probe in **D** abrogates the heparin staining of the secretory granule (G). A, x 43,000; B, x 48,000; C, x 79,000; D, x 83,500

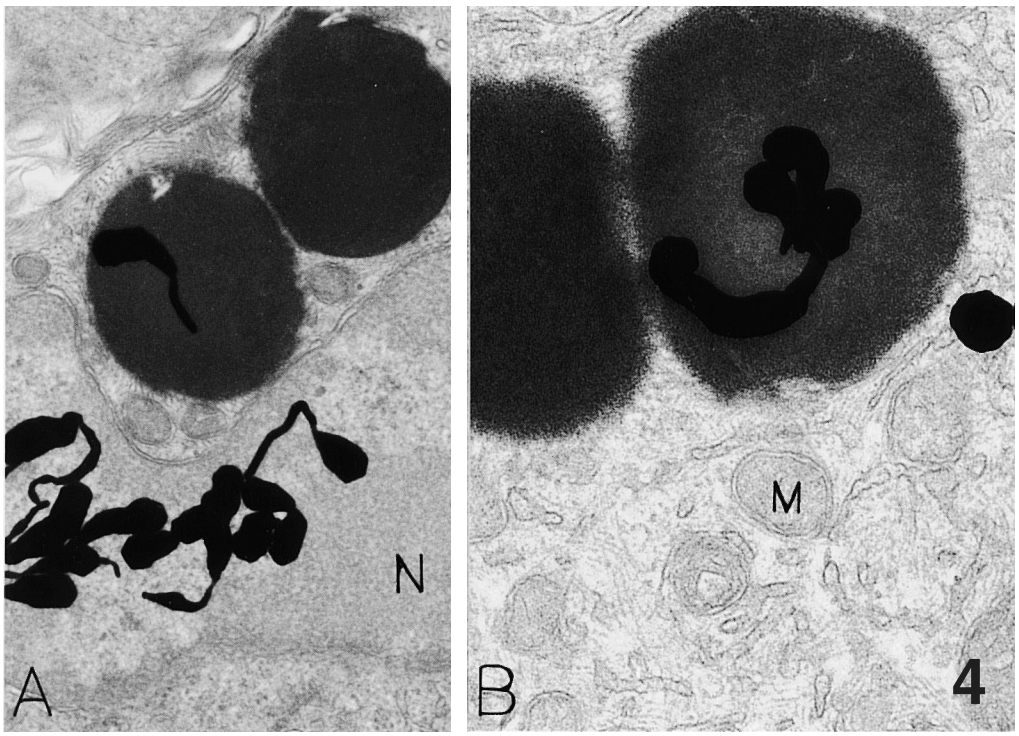

Fig. 4. [^{3}H]-uridine incorporation into HMC lipid body RNA. These ultrastructural autoradiographs of HMCs recovered in culture 6 hrs after degranulation show electron dense silver grains in the nuclear (N) matrix in **A** and in lipid bodies in **A**, **B**. One cytoplasmic silver grain is also present (B). M : mitochondria. A, x 36,000; B, x 55,000

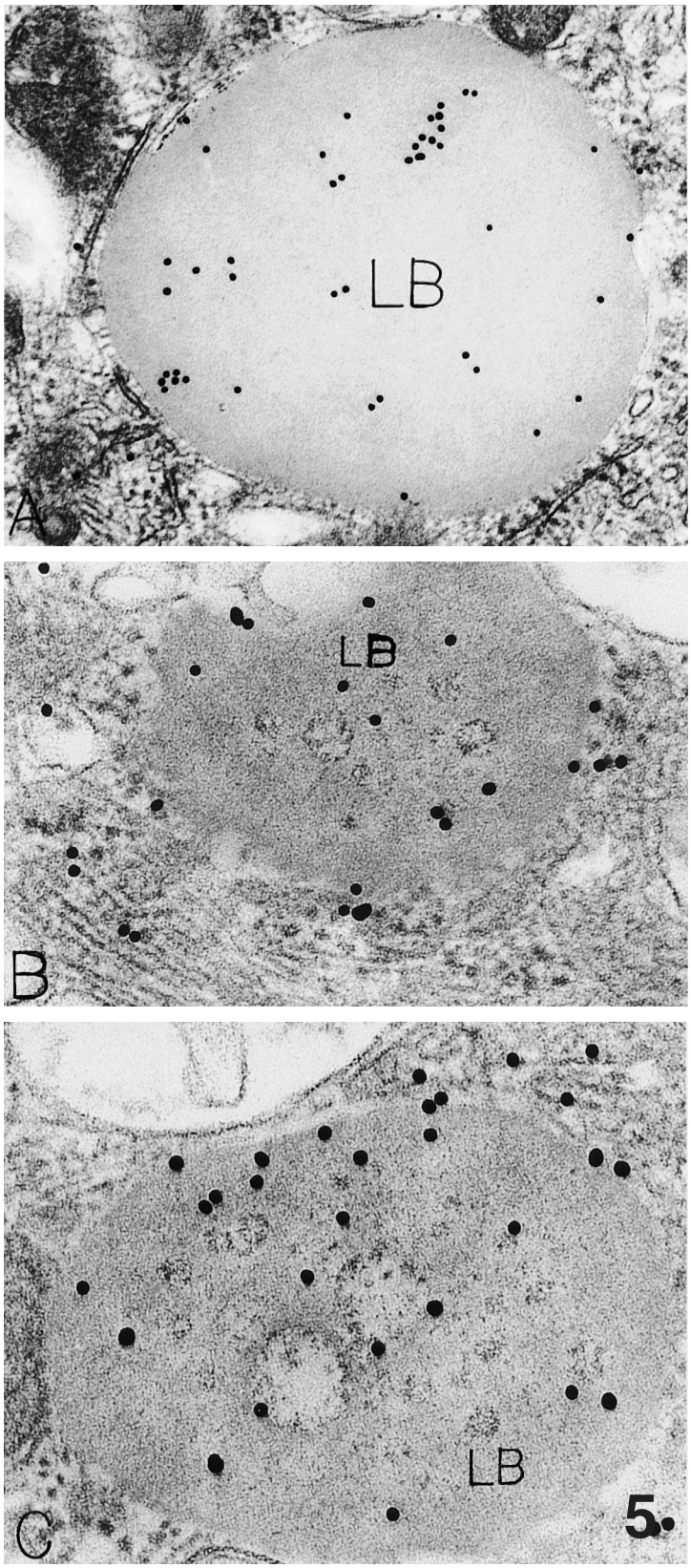

Ultrastructural immunogold imaging of uridine in human mast cell lipid body RNA

We used a postembedding immunogold procedure to label uridine (Dvorak and Morgan, 2000b; Dvorak et al., 2000b), a requisite RNA precursor, in HMC lipid bodies (Figs. 5,6). We found that this approach complemented the autoradiographic approach in that these disparate methods both localized uridine-containing RNA in lipid bodies (Figs. 4-6) as well as bound to free ribosomes (Fig. 6) and membrane-bound ribosomes (Fig. 7) and to RNA-rich nuclear domains (Fig. 8). As noted in earlier studies, HMC granules also contained immunogold label for uridine (Fig. 8a) (Dvorak and Morgan, 2000b; Dvorak et al., 2000b). Variable unmasking procedures showed that the hyaluronidase method (Qu et al., 1998a,b) regularly allowed immunogold detection of uridine in lipid bodies (Figs. 5, 6, 8) but unmasking with sodium metaperiodate (Dvorak et al., 1988a), Triton-X, or heparitinase did not. Positive controls included rough endoplasmic reticulum (RER)-rich plasma cells, which bound the uridine label to their membrane-attached ribosomes (Fig. 7c). When the specific primary antibody was omitted (Fig. 7a) or an irrelevant serum, or antibody was substituted for it, lipid bodies did not label. For an absorption control, we passed the specific anti-uridine antibody over poly(U) beads prior to staining the grids. This procedure prevented the staining of all known RNA-containing organelles as well as secretory granules and lipid bodies (Fig. 7b).

Anti-uridine stained lipid bodies were closely adjacent to elements of smooth endoplasmic reticulum (SER), (Fig. 5a), RER, free ribosomes (Figs. 5b, 6, 8a), and intermediate filament bundles that were also labeled for uridine (Figs. 5b,c, 6). Collections of free ribosomes nearby were heavily labeled (Fig. 6). Lipid bodies intimately associated with perinuclear membranous boundaries contained uridine-labeled RNA (Fig. 8). In some instances, linearly aligned gold particles filled the visible space between lipid body surfaces and the endoplasmic reticulum-invested perinuclear cisterns (Fig. 8).

Lipid bodies with visible internal vesicular and electron dense structures were present regardless of the unmasking procedures used. These vesicle-like

Fig. 5. Immunoreactive uridine in HMC lipid bodies. These immunogold preparations of 6 hr cultured control HMCs demonstrate RNA in lipid bodies (**A-C**), in LB matrix vesicles (**C**), in smooth endoplasmic reticulum next to a lipid body **(A)**, and in ribosomes and intermediate filaments which encase lipid bodies **(B, C)**. The unmasking procedure for these images was hyaluronidase (see materials and methods). LB = lipid body. A, x 51,000; B, x 84,000; C, x 98,000

structures, when present, particularly bound the anti-uridine label to their surfaces indicating the presence of RNA in these sublipid body domains (Fig. 5c). In experiments where uridine incorporation into lipid bodies had been previously assessed with autoradiography, we noted enhanced expression of immuno- reactive uridine in lipid bodies with the immunogold method. This was particularly evident when previously degranulated human mast cells were studied during late (e.g. 6 hr) recovery intervals compared to control cells.

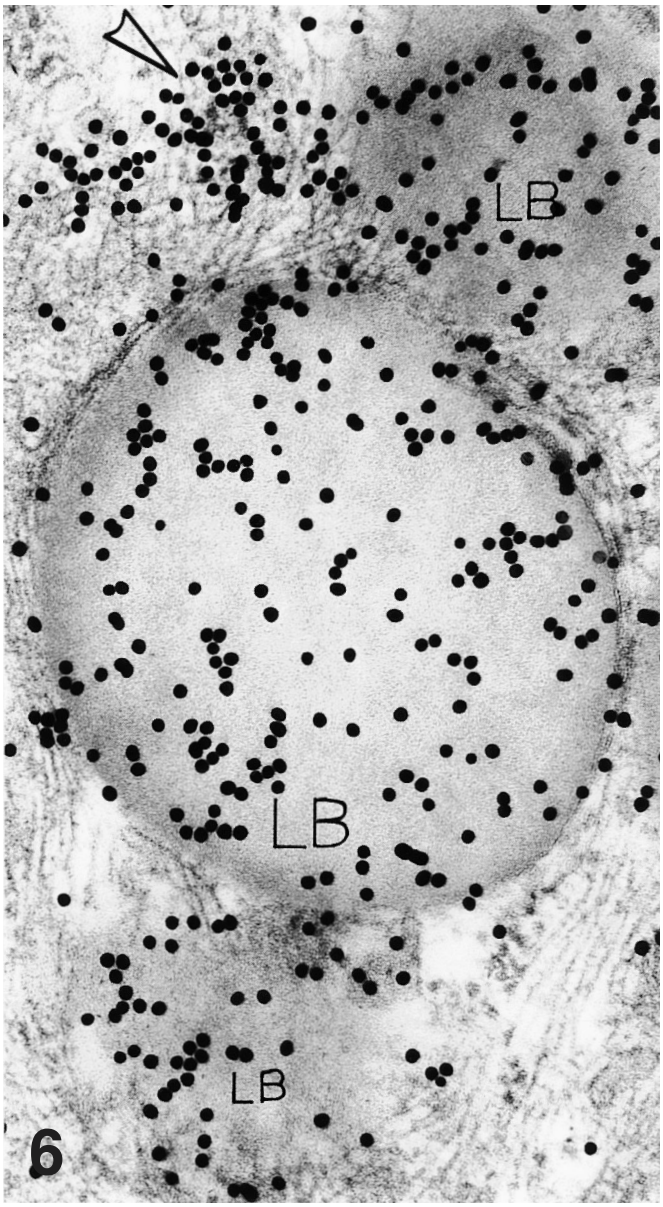

Fig. 6. Immunoreactive uridine indicating RNA in a HMC recovered in culture 6 hr after degranulation. Note extensive labeling of three cytoplasmic lipid bodies (LB) encased in intermediate filaments studded with ribosomes. A large cytoplasmic collection of ribosomes is also extensively labeled (arrowhead). x 80,000

Ultrastructural cytochemical, immunocytochemical and in situ hybridization methods with polyuridine probes detect mRNA in human mast cell lipid bodies

ISH with [^{3}H]-poly(U) *en grid* resulted in autoradiographic grains overlying HMCs. We previously reported that expected nuclear and cytoplasmic RNA-rich sites and organelles were labeled (Dvorak and Morgan 2000a; Dvorak et al., 2000b). Additionally, we described a new secretory granule localization of this probe indicating granule stores of poly(A) positive mRNA (Dvorak and Morgan 2000a; Dvorak et al., 2000b). We report here that the autoradiographic detection of [^{3}H]-poly(U) extends to lipid bodies (Fig. 9a,b) in HMCs indicating the presence of mRNA in these organelles as well.

Direct binding of the probe, poly(U)-gold (as well as binding after ISH) to lipid bodies was demonstrated (Fig. 9c). Both fused, electron dense, lipid bodies (Fig. 9c) and fused lipid bodies illustrating an internal honeycombed pattern had poly(U)-gold bound to them. Passage of poly(U)-gold over poly(A) beads before exposing the sample to poly(U)-gold removed lipid body labeling.

The biotinylated poly(U) probe labeled subcellular structures in HMCs. To test the authenticity of this labeling, two independent ISH protocols (Capco and Jeffery, 1978; Binder et al., 1986) were used as well as four independent reporter systems (Capco and Jeffery, 1978; Bendayan and Zollinger, 1983; Binder et al., 1986; Hiriyanna et al., 1988) for imaging the biotinylated poly(U) bound to mRNA in subcellular locations of human mast cells. The impact of proteinase K digestion, omission of hybridization and specific controls for the individual reporter systems were also evaluated. These data show that, with an ISH protocol, the photobiotinylated poly(U) probe consistently labeled the nuclear, cytoplasmic, granular (Dvorak and Morgan, 2000a) and lipid body compartments (Figs. 10a.b, 11a) of HMCs. Quantitative evaluation (Dvorak and Morgan, 2000a) revealed that the lipid body compartment label significantly exceeded that for mitochondria, another cytoplasmic organelle in HMCs ($p<0.001$). When the ISH protocol was omitted to determine the ability of the biotinylated poly(U) probe to bind directly to the samples, similar overall trends to those with ISH occurred. When samples without ISH were examined with or without proteinase K digestion, very little difference was noted in labeling.

We quantitated the gold label in human mast cells imaged with a second reporter system - protein A-gold - after the ISH protocol and in omission controls where the goat antibiotin antibody was deleted or the biotinylated poly(U) probe was deleted (Fig. 10c). With protein A-gold after the ISH protocol and exposure to the biotinylated poly(U) probe, granule (58%) and lipid

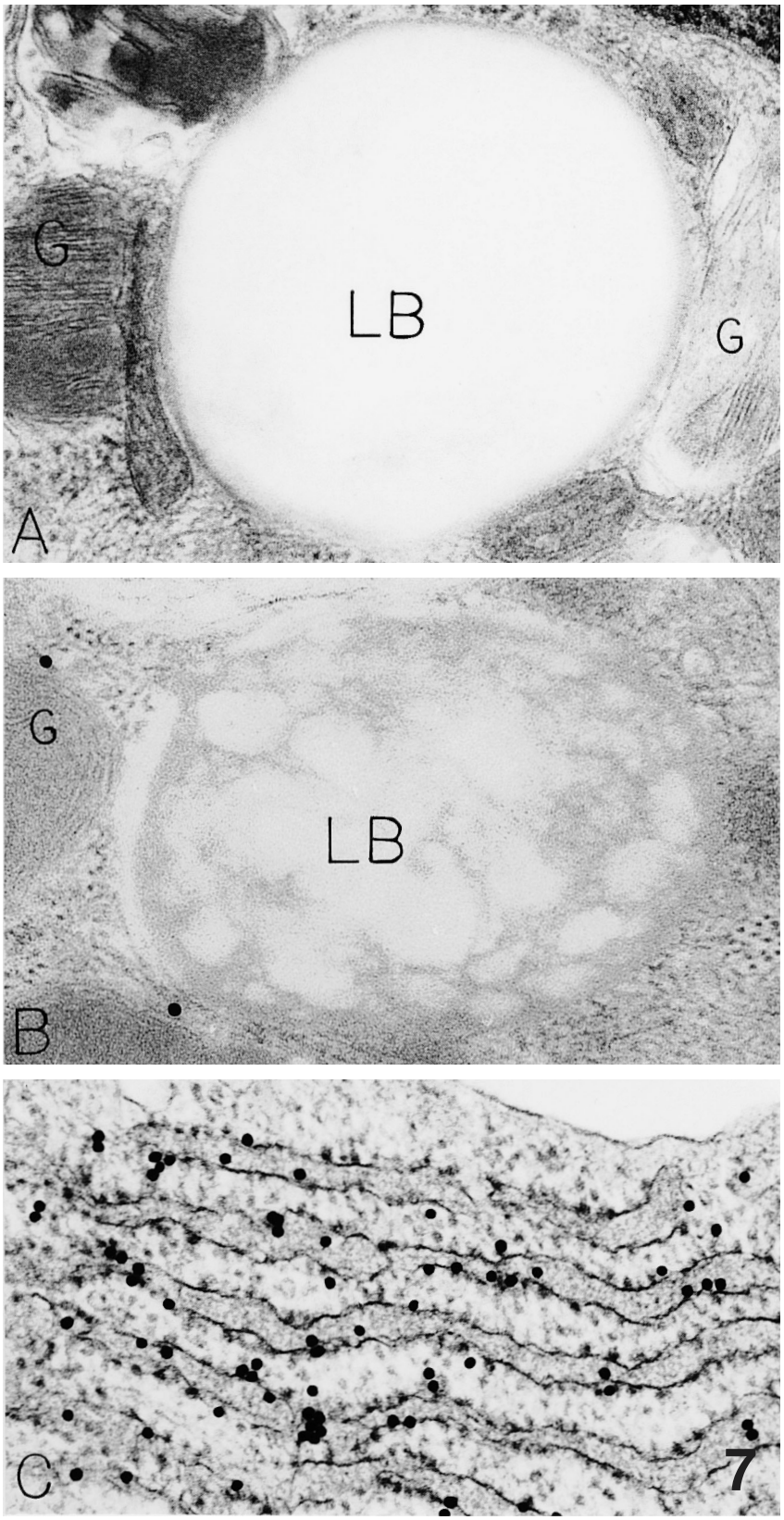

Fig. 7. Controls for the anti-uridine immunogold stain of 6 hr cultured HMCs **(A,B)** and immunoreactive uridine in a plasma cell also present in the culture **(C)**. In A, the specific anti-uridine antibody was omitted. No gold particles bind to the lipid body (LB), granules (G) or to cytoplasmic ribosomes nearby. In **B**, the specific antibody to uridine was absorbed with polyuridine before staining the sample. The LB and G are not labeled. In **C**, the parallel arrays of rough endoplasmic reticulum with attached ribosomes are labeled with gold particles indicating their RNA content. This plasma cell serves as a good positive control since it was present in the cultured HMCs used for these studies. LB: lipid body; G: granule. A, x 54,000; B, x 72,000; C, x 73,000

body (44%) label exceeded Epon background (2%) ($p<0.001$); granule label exceeded that of lipid bodies ($p<0.001$) (Dvorak and Morgan, 2000a). Use of either streptavidin-gold or goat-antibiotin-gold (Fig. 11a) as reporters also labeled human mast cell lipid bodies.

A variety of controls were quantitated to evaluate specificity of the electron microscopic ISH using the biotinylated poly(U) probe. When the biotinylated poly(U) probe or the biotinylated poly(U) probe plus the primary antibody to biotin were omitted, lipid body label was eradicated. Thus, the Photoprobe (long arm) biotin was essential to image mRNA in human mast cell lipid bodies, and the gold-labeled secondary antibody did not artifactually bind to the samples but was specifically bound to biotin in the poly(U) probe. When the primary antibiotin antibody was omitted using the protein A-gold reporter system, protein A-gold did not bind to the biotinylated poly(U) probe (but did increase background levels of label). When the biotinylated poly(U) probe was omitted, the primary antibody to biotin did not stick

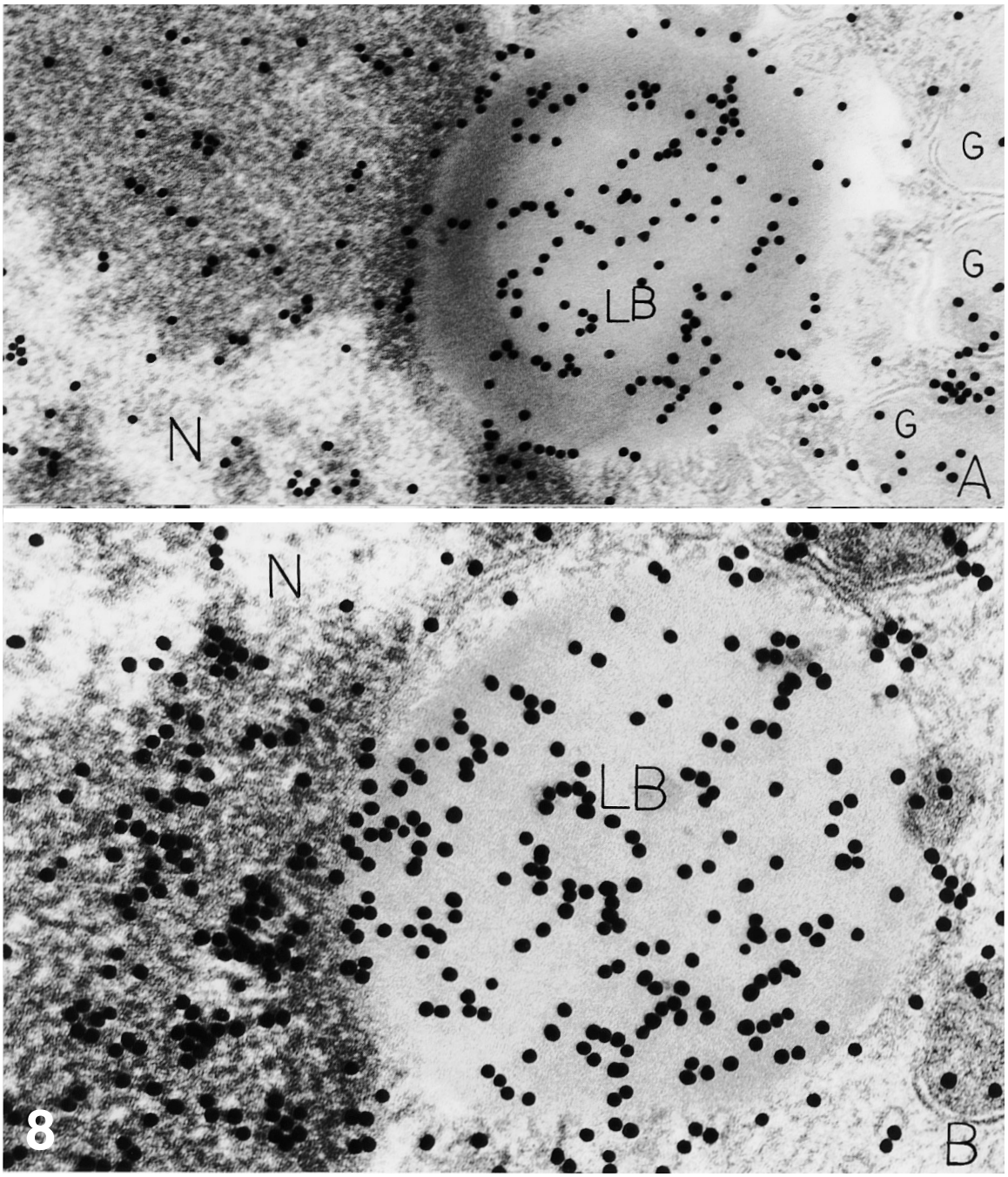

Fig. 8. 6 hr control cultured HMC lipid bodies (LB) show immunoreactive uridine indicating RNA. These preparations were unmasked with hyaluronidase and show intensively labeled nuclei (N), LBs, and granules (G). Note the linear array of gold particles along LB surfaces and intensive packing of label at the LB-nuclear interface in the region of the nuclear membranes and perinuclear cisternae. LB: lipid body;
N: Nucleus.
A x 80,000;
B x 99,000

to human mast cells, and when the biotinylated poly(U) probe and the primary antibiotin antibody were omitted, protein A-gold did not stick to the sample (Fig. 10c). Omission of the biotinylated poly(U) probe in conjunction with the streptavidin-gold or goat-antibiotin-gold reporters also was negative (Fig. 11b).

A BSA-poly(U)-gold probe was constructed for use in localizing mRNA by electron microscopic ISH. The probe was made by cross-linking BSA to poly(U) with glutaraldehyde, preparing a colloidal gold suspension, and attaching the BSA-poly(U) to gold. This general probe for mRNA labeled the granular, nuclear, cytoplasmic (Dvorak and Morgan, 2000a) and lipid body compartments (Fig. 12b) in human mast cells isolated from surgically removed lung specimens. To make this determination, we evaluated a number of procedural variations in three different ISH protocols as well as in a number of controls (to properly evaluate the lipid body compartment, we found that the short ISH protocol was needed since the long protocol generally extracted lipid body content from samples (Fig. 12a).

Controls included BSA-gold with and without ISH (the BSA used for conjugation to gold was treated with glutaraldehyde identically to the treatment for cross-linking BSA to poly[U]) and gold alone with and without ISH (Fig. 12c). These controls showed markedly reduced attachment to subcellular compartments of human mast cells compared to samples exposed to the BSA-poly(U)-gold probe. Generally, Epon background gold counts were increased after ISH schedules, compared to direct binding of the probe in the absence of ISH. Increased Epon background was similarly noted when the control BSA-gold probe underwent ISH.

A less destructive procedure for imaging ISH of lipid bodies was devised. This involved hybridization (short protocol) with unlabeled poly(U) and subsequent imaging specifically bound poly(A)-positive mRNA label with a specific antibody to uridine and a gold labeled secondary antibody directed toward the primary anti-uridine antibody. With this procedure, expected

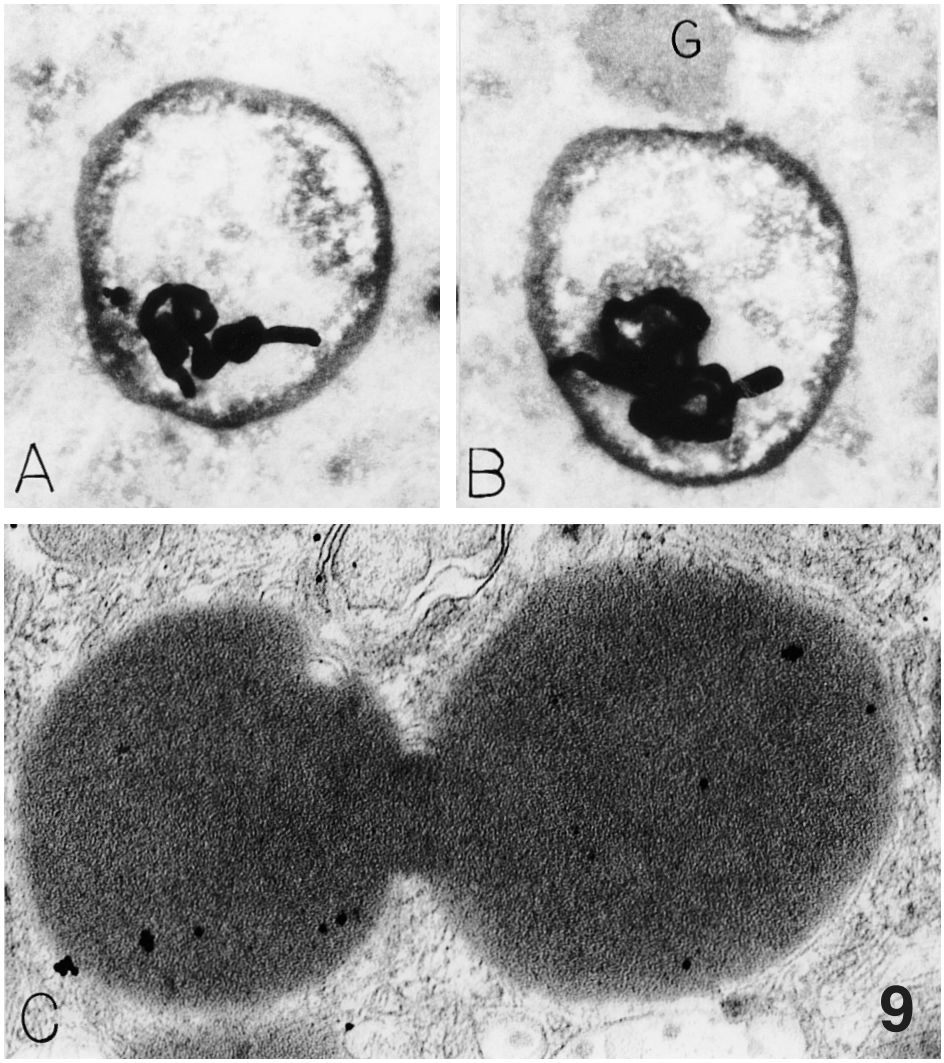

Fig. 9. 6 hr ctrol cultured HMC lipid bodies show label indicating poly(A)-positive mRNA. In A and B, auto-radiographs of tritiated poly(U) hybridized to the samples show silver grains overlying lipid bodies. The samples were not osmicated or exposed to uranyl en bloc. This method of preparation preserves little of the osmiophilic lipid contents of LBs, leaving a thick electron dense outer shell to the organelle. G= granule. In **C**, a poly(U)-gold probe was used to directly stain the lipid bodies which are joined by a narrow lipid-rich fusion area between them. This is a standard ultrastructural sample (compare with panels A, B). A,B x 52,000; C, x 77,000

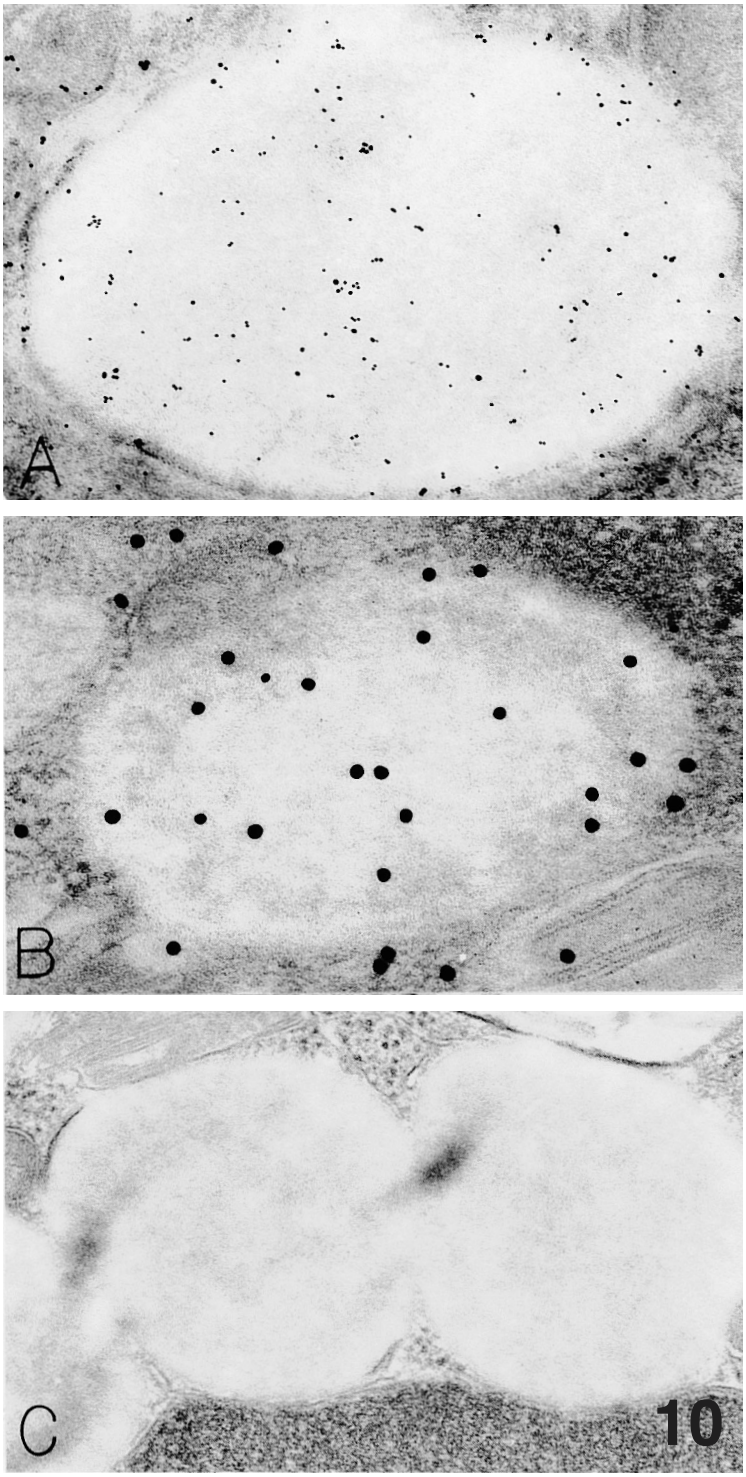

Fig. 10. 6 hr control cultured HMC lipid bodies show label indicating poly(A)-positive mRNA. In **A** and **B**, ISH of biotinylated poly(U), imaged with sequential incubation of an antibiotin antibody and gold-labeled protein A, shows gold particles overlying large lipid bodies. Panel **C**, is a control for protein A-gold sticking since ISH of the biotinylated poly(U) probe and the anti-biotin antibody were omitted. Lipid bodies are not labeled by protein A gold alone. A, x 52,000; B, x 79,000; C x 49,500

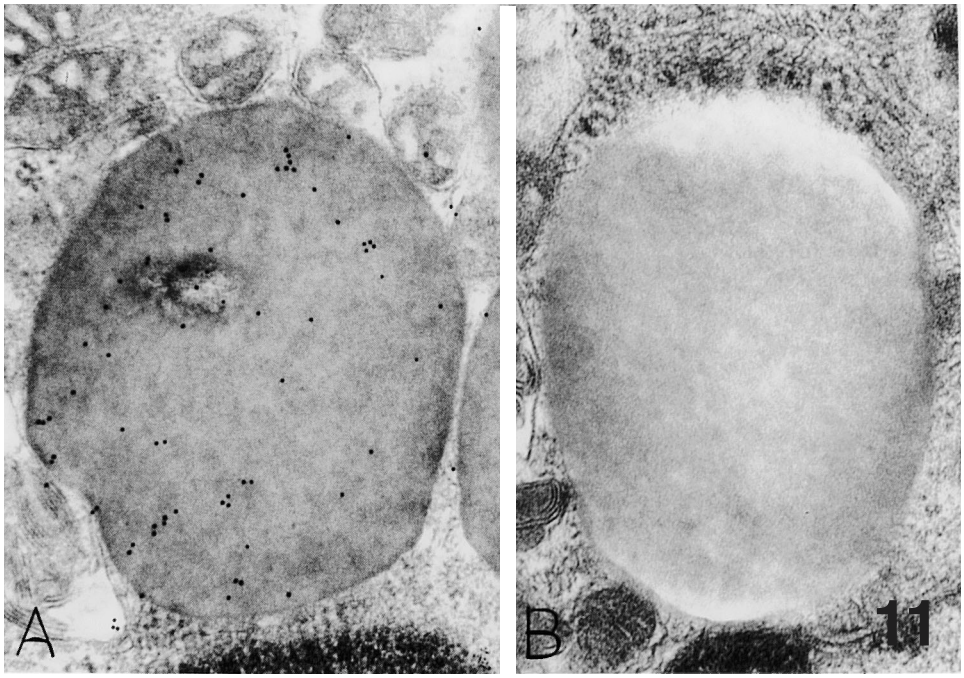

Fig. 11. Similar preparations of lipid bodies (to Figure 10) show poly(A)-positive mRNA. In this case the reporter system used after ISH of the biotinylated poly(U) probe was a gold-labelled anti-biotin antibody. The lipid body in panel **A** is labeled with gold particles; in panel **B**, the biotinylated poly(U) probe was omitted and the lipid body is not labeled by the gold-labeled reporter antibody. A, x 45,000; B, x 55,000

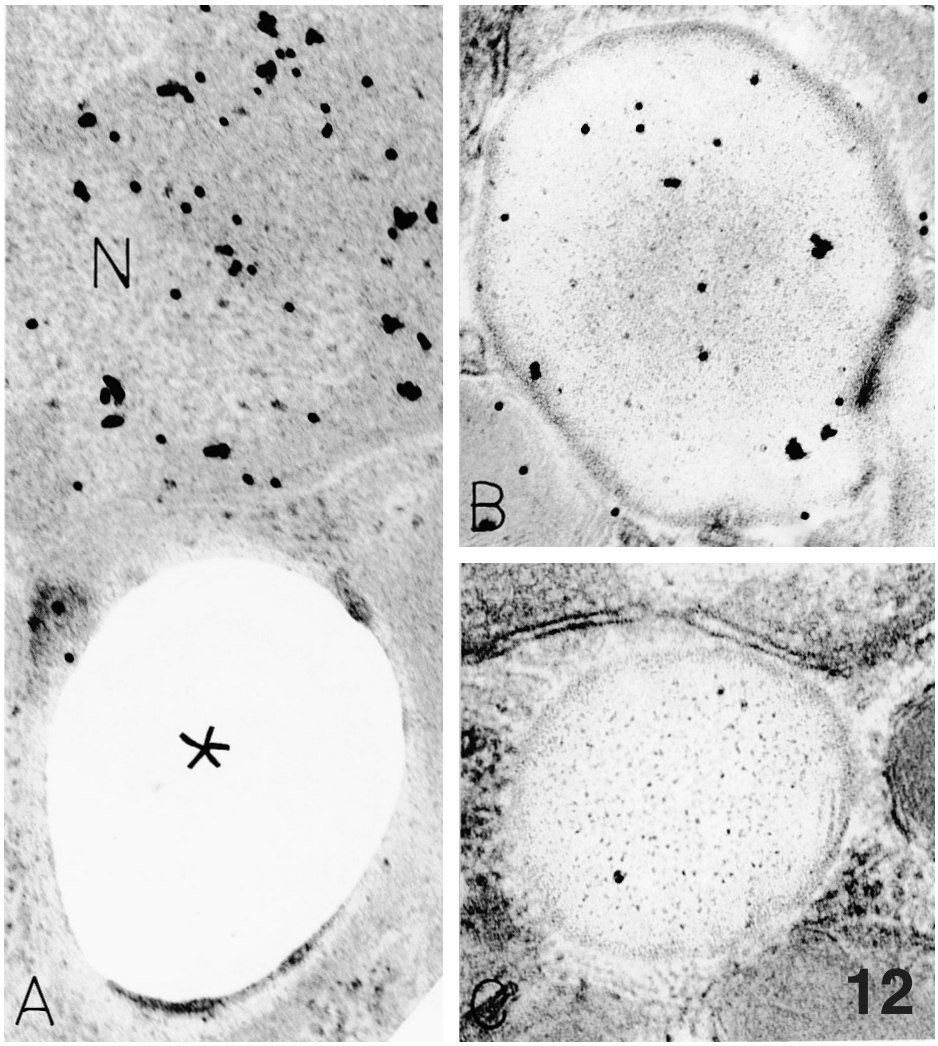

Fig. 12. ISH of 6 hr control cultured HMCs. The probe used here was BSA-poly(U)-gold. An overnight (long) ISH schedule was used in **A**. Note that the nucleus (N) is heavily gold labeled for poly(A)-positive mRNA and/or their precursors but that this destructive ISH schedule has caused the lipid body to be torn from the thin section leaving roled up edges of lipid material to surround the empty LB-sized space (star). **A** short (3.5 hr) ISH schedule was used in panels **B and C**, either with the BSA-poly(U) gold probe present **(B)** or absent **(C)**. In the short ISH schedule LBs are not destroyed **(B, C)** and when the specific probe is present lipid bodies bind it as indicated by gold particles overlying the LB in panel B. Omission of the probe abrogates LB label, as in panel **C**. A, x 88,000; B, x 83,500; C, x 92,500

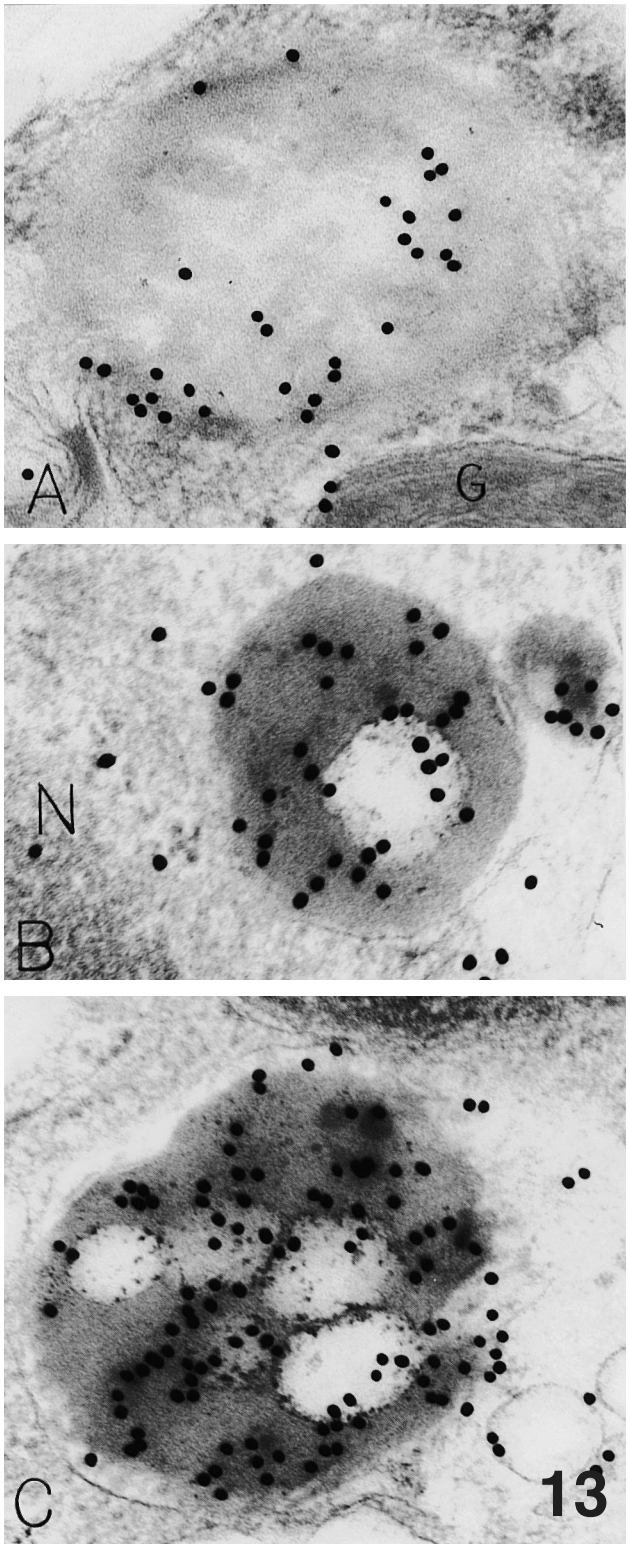

Fig. 13. ISH of 6 hr control cultured HMCs slow poly(A)-positive mRNA in LBs. The probe used here for hybridization was unlabeled poly(U) that was visualized by an immunogold reporter. The short hybridization schedule allowed excellent preservation of LBs, which illustrate overlying gold particles in all panels. Intralipid body vesicles (panels **B, C**) are also gold-labeled indicating the presence of poly (A)-positive mRNA. N: nucleus; G: granule. A, x 74,000; B, x 84,000; C, x 74,000

mRNA-containing structures, secretory granules and lipid bodies (and their internal vesicular substructures) were labeled indicating the presence of poly(A)-positive mRNA (Fig. 13).

Ultrastructural immunogold cytochemistry of HMCs with specific autoimmune human sera detects RNA-associated protein antigens of different RNA species in and associated with lipid bodies.

Specific autoimmune human sera from two sources were used (Figs. 14-16); each was verified for specificity (see Materials and Methods). Previously we showed that HMC nuclei and granules were stained with the specific human antisera (Dvorak and Morgan, 2000b). Using a similar approach, we show here that HMC lipid bodies also were stained with the immunogold procedure with human sera specific for Ro (Fig. 14a, b), a small cytoplasmic RNP, subclass of La; for La (Fig. 14c), precursors of 5s ribosomal RNA and tRNA; for RNP (Fig. 15a), indicating U1, a snRNA essential for splicing (Hinterberger et al., 1983; Padgett et al., 1983; Kramer et al., 1984; Pettersson et al., 1984); for Sm (Fig. 14d), indicating U2, U5, U4/U6 snRNAs; and for P (Fig. 16a,b), representing three phosphoproteins (called P0, P1, P2) of the 60S ribosomal subunit. Perigranular ribosomes also were labeled with the sera specific for the ribosomal P antigen.

Controls for the specificity of the granule and ribosome labeling with specific autoantibody-containing human sera were done. These included omission of specific primary antibody (Fig. 16c), substitution of NHS for the specific primary antibody (Fig. 15b), substitution of an irrelevant autoantibody-containing human serum specific for mitochondria for the primary antibody (in this case, this positive control included specifically labeled mitochondria, whereas lipid bodies were negative).

Variable combinations of unmasking procedures for these stainings were done. In this case, sodium metaperiodate provided the best unmasking results and was used to demonstrate RNP, Sm, Ro, and La. Ribosomal P antigen was readily demonstrable with either sodium metaperiodate, with hyaluronidase (Fig. 16a,b), or with combinations of the unmasking procedures.

Discussion

The distribution of ribosomes in mature human mast cells, a major granulated secretory cell, does not resemble that in other secretory cells, such as pancreatic acinar cells and plasma cells. By routine ultrastructural analysis, ribosomes in human mast cells are often close to, attached to, or even appear to be within secretory granules and lipid bodies. To document better these relationships, we used multiple electron microscopic imaging methods, based on different principles, to define RNA, ribosome, and lipid body relationships in mature

human mast cells. These methods included ribonuclease-gold affinity staining, EDTA regressive staining, immunogold labeling of ribonucleoproteins or uridine, direct binding or binding after ultrastructural in situ hybridization of various polyuridine probes to polyadenine in mRNA, and ultrastructural autoradiographic localization of [3H]-uridine incorporated into cultured human mast cells. These different labeling methods demonstrated ribosomes, RNA, ribonucleoproteins associated with small nuclear ribonucleic acids and ribosomes, mRNA, and uridine to be associated with secretory granules and lipid bodies in human mast cells, implicating both organelles in a larger synthetic role in mast cell biology.

The findings that are presented here are analogous to those we have reported in detail earlier tying RNA and

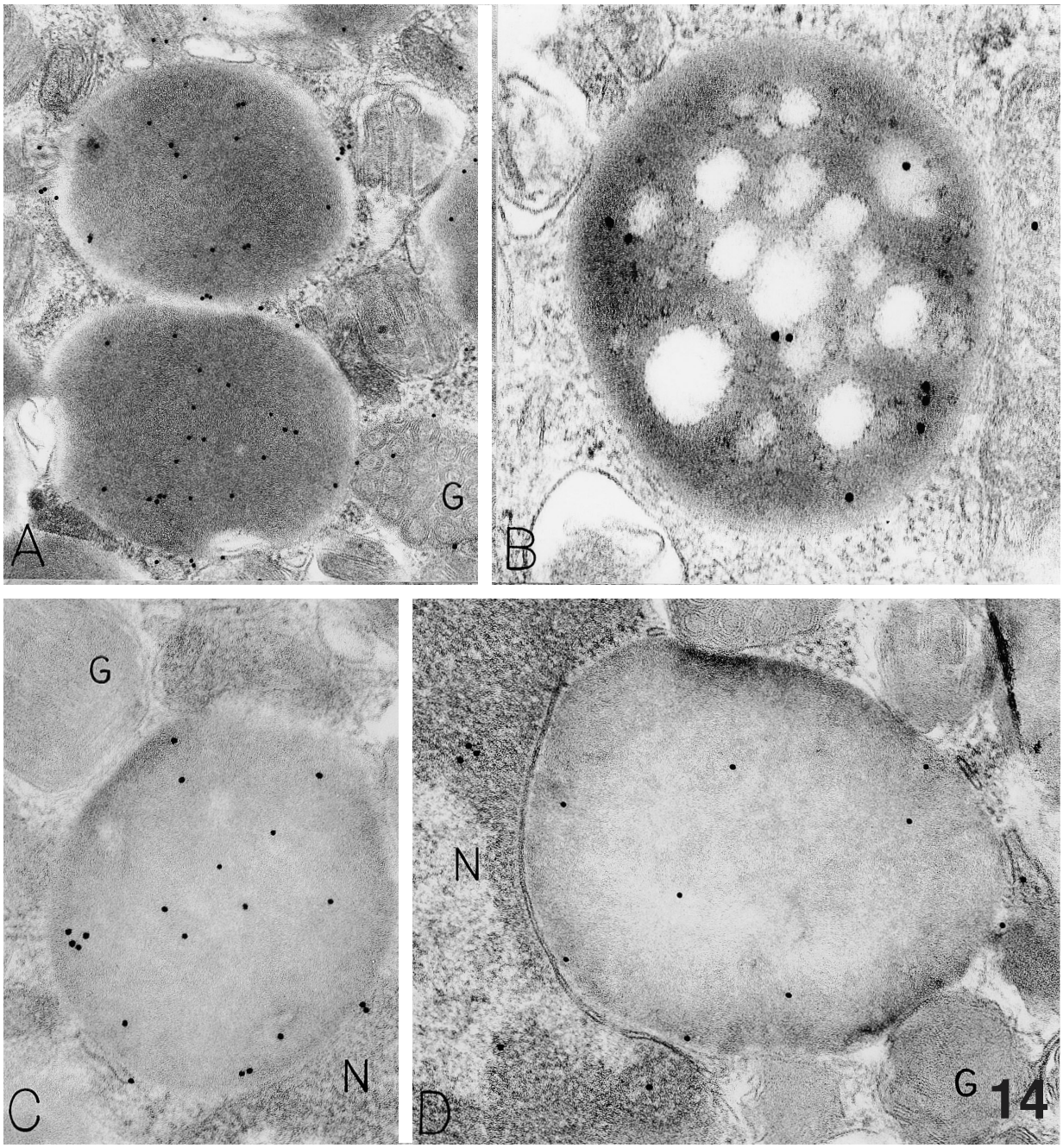

Fig. 14. Immunogold studies with specific human autoimmune sera show gold labelled LBs in 6 hr control cultured HMCs. Sea with specificity for Ro (A, B), IA (C), SM (d) label cytoplasmic LBs. N: nucleus; G: granule. A, x 43,000; B, x 76,500; C, x 62,000; D, x 58,500

secretory granule biology in HMCs together (reviewed in Dvorak and Morgan, 2002).

Initially we used an enzyme affinity technique (Bendayan, 1981) to identify RNA by binding RNase-

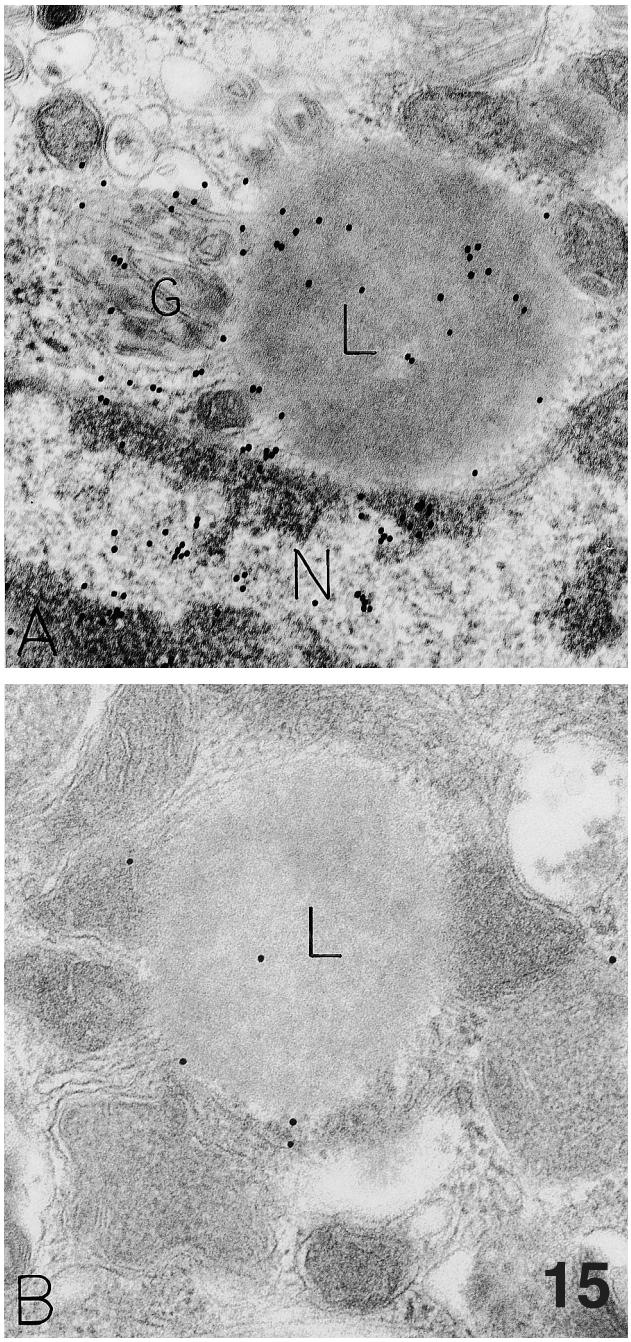

Fig. 15. Similar preparations of lipid bodies (to figure 14). Human autoimmune sera with specificity for RNP **(A)** label the large lipid body (L), the secretory granule (G) beside it and the nucleus (N) beneath it. When normal human sera (NHS) was substituted for the specific autoimmune sera, in **B**, only three gold particles bind to the lipid body (L). A, x 49,500; B, x 53,000

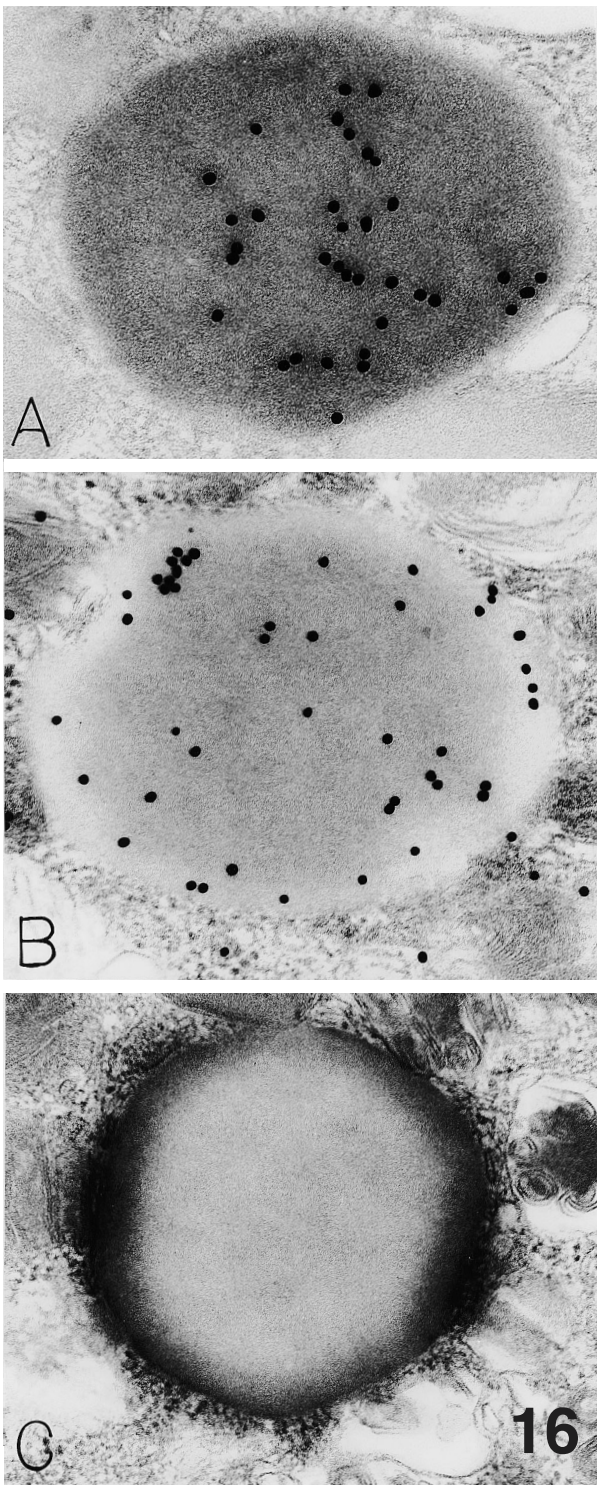

Fig. 16. Immunogold studies with specific human autoimmune sera for P show extensively gold labeled lipid bodies in panels **A, B;** omission of the specific antisera abrogates lipid body label in **C**. A x 66,000; B, x 58,000; C, x 59,000

gold to section surfaces (Dvorak and Morgan, 1998, 1999). This method avidly labeled mast cell granules (and cytoplasmic ribosomes) (Dvorak and Morgan 1998). Extensive controls for this technique revealed an avidity of RNase-gold for human mast cell granule heparin (Dvorak and Morgan, 1998). Quantitative studies of RNA blocking showed a reduction in granule label that did not achieve statistical significance, whereas those for heparin blocking did (Dvorak and Morgan, 1998). Human mast cell (HMC) granules store proteoglycans that have been shown primarily to consist of heparin (and smaller quantities of chondroitin sulfate E) (Stevens et al., 1988; Thompson et al., 1988), a macro-molecule said to be the most anionic substance in the body (Anderson and Wilbur, 1951; Salmivirta et al., 1996) and to be unique to mast cell granules (Lindahl and Höök, 1978; Salmivirta et al., 1996).

In samples of HMCs prepared similarly with RNase-gold staining, another prominent organelle, cytoplasmic lipid bodies, also were stained. Unlike the extensive studies showing that this staining indicated heparin in granules, lipid bodies appeared to bind the RNase-gold by virtue of contained RNA. That is, prior absorption of the reagent with heparin removed granule staining (e.g. heparin stores) but not lipid body staining, indicating RNA.

Thus, a new use for the ultrastructural enzyme affinity-gold method originally designed to detect RNA, i.e. to detect heparin in HMC granules, was found (Dvorak and Morgan, 1998). The studies also confirmed, as reported (Bendayan, 1981), that the method detects RNA in ribosomes and nucleoli of HMCs. These findings provide a new use for this enzyme affinity-gold method in mast cell studies – one derived from the known biochemical properties of heparin as an RNase inhibitor, and identify a new subcellular location for RNA in HMCs – in lipid bodies.

A modified EDTA-based regressive stain (Bernhard, 1969), which preferentially retains staining of RNP, while deoxyribonucleoprotein is bleached, was used to define important close associations of ribosomes and lipid bodies in mature HMCs. The method is thought to reflect ribosomal protein(s) that retain electron density with this stain. With it, ribosomes were detected adjacent and attached to lipid bodies.

These studies were extended by using human sera specific for ribosomal proteins (anti-P) (Elkon et al., 1985, 1986) as the primary antibody in immunogold staining. In this case, human mast cell lipid bodies and cytoplasmic ribosomes were labelled. Thus, each of these two disparate methods indicates that specific ribosomal proteins reside in HMC lipid bodies.

We used two different methods to show that HMC lipid bodies contain uridine, an integral ingredient of RNA species generally. Initially, we localized uridine to lipid bodies with ultrastructural autoradiography. The immunogold detection of uridine with an antibody specific for uridine, in lipid bodies was also done. These two disparate means of detection leave little doubt that human mast cell lipid bodies contain uridine, which is integral to all RNA species.

We used direct binding and ultrastructural ISH of general poly(U) probes, prepared in diverse ways, to detect poly (A)-positive mRNA stores in human mast cells (Dvorak et al., 2000b; Dvorak and Morgan 2000a). These methods demonstrated that poly(A)-positive mRNA species were contained not only in the expected nuclear and cytoplasmic sites but also in the secretory granules and lipid bodies of human mast cells. RNA processing in the nucleus involves splicing of precursor mRNAs, polyadenylation of pre-mRNAs, and transport of specific mRNAs from nucleus to cytoplasmic sites – mRNAs that associate with cytoplasmic ribosomes to direct specific protein syntheses (Perry, 1981; Mattaj, 1990; Mehlin et al., 1992; Gray and Cedergren, 1993). The electron microscopic ISH localizations of granule and lipid body stores of poly(A) – containing mRNAs, as well as nuclear stores of poly(A)-containing precursors of mRNA, indicate that site-specific localization of mRNAs in cytoplasmic secretory granule and lipid bodies (in addition to cytoplasmic ribosomes) exist.

We localized small nuclear RNAs involved in splicing of pre-mRNAs to produce mRNAs for subsequent protein synthesis. The snRNAs were localized by immunogold staining with specific human antisera. They are uridine-rich (Busch et al., 1982) and, thus, would be imaged with our (5,6-^{3}H)-uridine (Dvorak et al., 2000a,b) and anti-uridine studies (Dvorak and Morgan 2000b), but they do not contain poly(A) (Busch et al., 1982) and, thus would not be imaged with the poly(U)-based methods which we used (Dvorak and Morgan, 2000a). The human antisera to snRNPs are present in patients with certain autoimmune diseases (Schur et al., 1967; White and Hoch 1981; Conner et al., 1982; Hardin et al., 1982; Tan, 1991; Steiner et al., 1996). Sera containing antibody to Sm are specifically present in patients with systemic lupus erythematosus and, in the antisera that we used, are reactive with polypeptides shared by U2 and U4-6 snRNP (Conner et al., 1982). Sera containing antibody to RNP are present primarily in patients with mixed connective tissue disease; the sera we used were specific for proteins associated only with U1 snRNP. U1 has been specifically implicated as essential in the splicing of mRNA precursors (Mount et al., 1983; Padgett et al., 1983; Krämer et al., 1984; Ruby and Abelson, 1988; Heinrichs et al., 1990; Kuo et al., 1991). Thus, small RNPs, important in the processing of mRNA precursors, are located in human mast cell lipid bodies, as well as in expected nuclear sites. It has been suggested previously that these snRNAs actually spend brief periods in the cytoplasm, prior to returning to the nucleus where they are long-lived (Eliceiri and Gurney 1978, Patton and Wieben, 1987). Specifically, cytoplasmic sites of U 1 RNA processing and RNP assembly have been proposed (Madore et al., 1984). Our data suggest that human mast cell lipid bodies may be one such site.

We also tested human sera containing antibodies to Ro and La (Hendrick et al., 1981; Elkon and Culhane, 1984; Woline and Steitz, 1984; McNeilage et al., 1985; Ben-Chetrit et al., 1988; St. Clair, 1992; Simons et al., 1994; Farris et al., 1997). These are present primarily in patients with Sjögren's syndrome. Our sera for Ro were specific, being nonreactive to La, RNP and Sm; but the sera for La had low reactivity with Ro as well. These small RNPs are said to be primarily cytoplasmic (Ro) or nuclear (La), but no localization studies for lipid bodies have been reported. A possible role for Ro in translation of subsets of mRNAs in heart and brain has been proposed (Wolin and Steitz 1984); nucleoli and ribosome-rich cytoplasmic cellular regions suggested to other investigators a role (s) in ribosome synthesis, assembly or transport (Farris et al., 1997). Thus, our localization of Ro in human mast cell lipid bodies adds this location to the possible repertoire for this small cytoplasmic (scy) RNP.

La, another small RNP, recognized by antiserum to La, labels precursor forms of 5S ribosomal rRNA and certain transfer (t) RNAs (e.g., those for the amino acids Met, Asp, Gly, Glu, Asn) (Rinke and Steitz, 1982). Initially thought to be a snRNP, La has been localized to nucleolar and cytoplasmic sites, particularly to rough endoplasmic reticulum and to polyribosomes. Cytoplasmic RNAs bound to La include the signal recognition particle (srp) RNA. Proposed functions of this small RNP include involvement in protein synthesis via tRNAs and the srpRNA, modulation of mRNA translation, participation in functional aspects of the biogenesis of polymerase III-transcripts, and in ribosomal biosynthesis in the nucleolus (Rinke and Steitz, 1982; Bachmann et al., 1987; Yoo and Wolin, 1997; Sobel and Wolin, 1999). Our immunoelectron microscopic localization of La in human mast cell lipid bodies (with positive nuclear labeling) identifies additional RNA species in the lipid body location.

A large body of evidence has recently defined RNA transport and localization as a mechanism for facilitating site-specific synthesis at various subcellular organelles in cells of diverse origin from multiple species (Gottlieb, 1990; Singer, 1992, 1993; Wilhelm and Vale, 1993; Bassell and Singer, 1997; Bassell et al., 1999; Etkin and Lipshitz, 1999; Jansen, 1999; Lasko, 1999; Mowry and Cote, 1999). Such traveling RNA has been intimately associated with all three major cytoskeletal elements, i.e., microfilaments, intermediate filaments and microtubules (Lenk et al., 1977; Fulton et al., 1980; Ornelles et al., 1986; Isaacs and Fulton, 1987; Gottlieb, 1990; Singer, 1992; Bassell, 1993; Bassell and Singer, 1997; Mowry and Cote, 1999), and specific zip codes for localizing individual mRNAs at subcellular sites have been postulated (Singer, 1992; Hill et al., 1994; Kislauskis et al., 1994; Etkin and Lipshitz, 1999). Lipid bodies have not been considered as such a site, but the evidence that we present suggests that they must also be included in the travels of mRNA (Wilhelm and Vale, 1993; Knowles et al., 1996) in mast cell biology.

Acknowledgements. Supported by National Institutes of Health Grants AI 33372 & AI 22571.

References

Anderson N.G. and Wilbur K.M. (1951). Studies on isolated cell components. II. The release of a nuclear gel by heparin. J. Gen. Physiol. 34, 647-656.

Angelier N., Bouteille M., Charret R. Curgy J.-J., Delain E., Fakan S., Geuskens M., Guelin M., Lacroix J.-C., Laval M. Steinert G. and Van Assel S. (1976). Detection of nucleic acids by means of ultrastructural autoradiography. J. Microsc. Biol. Cell. 27, 215-230.

Asboe-Hansen G. (1971). Mast cells and the skin. In: E.B. Helwig & F. K. Mostofi (eds). Williams & Wilkins Co. Baltimore. pp 83-111.

Avrameas S. (1969). Coupling of enzymes to proteins with glutaraldehyde. Use of the conjugates for the detection of antigens and antibodies. Immunochemistry 6, 43-52.

Bachmann L. and Salpeter M.M. (1965). Autoradiography with the electron microscope. A quantitative evaluation. Lab. Invest. 14, 1041-1053.

Bachmann M., Pfeifer K., Schröder H.C. and Müller W.E.G. (1987). The nucleocytoplasmic shuttling of the La antigen in CV-1 cells. Mol. Biol. Rep. 12, 239-240.

Barth J.A., Li W., Krasinski S.D., Montgomery R.K., Verhave M. and Grand R.J. (1998). Asymmetrical localization of mRNAs in enterocytes of human jejunum. J. Histochem. Cytochem. 46, 335-343.

Bassell G. and Singer R.H. (1997). mRNA and cytoskeletal filaments. Curr. Opin. Cell Biol. 9, 109-115.

Bassell G.J. (1993). High resolution distribution of mRNA within the cytoskeleton. J. Cell. Biochem. 52, 127-133.

Bassell G.J., Oleynikov Y. and Singer R.H. (1999). The travels of mRNAs through all cells large and small. FASEB J. 13, 447-454.

Beil W.J., Weller P.F., Peppercorn M.A., Galli S.J. and Dvorak A.M. (1995). Ultrastructural immunogold localization of subcellular sites of TNF-a in colonic Crohn's disease. J. Leukoc. Biol. 58, 284-298.

Ben-Chetrit E., Chan E.K.L., Sullivan K.F. and Tan E.M. (1988). A 52-kD protein is a novel component of the SS-A/Ro antigenic particle. J. Exp. Med. 167, 1560-1571.

Bendayan M. (1981). Ultrastructural localization of nucleic acids by the use of enzyme-gold complexes. J. Histochem. Cytochem. 29, 531-541.

Bendayan M. (1989). The enzyme-gold cytochemical approach: A review. In: Hayat M.A. (ed). Academic Press. San Diego, CA. pp117-147.

Bendayan M. and Zollinger M. (1983). Ultrastructural localization of antigenic sites on osmium-fixed tissues applying the protein A-gold technique. J. Histochem. Cytochem. 31, 101-109.

Bernhard W. (1969). A new staining procedure for electron microscopical cytology. J. Ultrastruct. Res. 27, 250-265.

Biggiogera M., Bottone M.G. and Pellicciari C. (1998). Nuclear RNA is extruded from apoptotic cells. J. Histochem. Cytochem. 46, 999-1005.

Biggiogera M. and Fakan S. (1998). Fine structural specific visualization of RNA on ultrathin sections. J. Histochem. Cytochem. 46, 389-395.

Binder M., Tourmente S., Roth J., Renaud M. and Gehring W.J. (1986). In situ hybridization at the electron microscope level: Localization of

transcripts on ultrathin sections of Lowicryl K4M-embedded tissue using biotinylated probes and protein A-gold complexes. J. Cell Biol. 102, 1646-1653.

Bozza P.T., Yu W., Penrose J.F., Morgan E.S., Dvorak A.M. and Weller P.F. (1997). Eosinophil lipid bodies: Specific, inducible intracellular sites for enhanced eicosanoid formation. J. Exp. Med. 186, 909-920.

Brooks E.M. and Binnington K.C. (1989). Gold labeling with wheat germ agglutinin and RNAse on osmicated tissue embedded in epoxy resin. J. Histochem. Cytochem. 37, 1557-1561.

Brown D.A. (2001). Lipid droplets: proteins floating on a pool of fat. Curr. Biol. 11, R446-449.

Busch H., Reddy R., Rothblum L. and Choi Y.C. (1982). SnRNAs, SnRNPs, and RNA processing. Annu. Rev. Biochem. 51, 617-654.

Capco D.G. and Jeffery W.R. (1978). Differential distribution of poly(A)-containing RNA in the embryonic cells of Oncopeltus fasciatus. Analysis by in situ hybridization with a [^{3}H]poly(U) probe. Dev. Biol. 67, 137-151.

Caro L.G., van Tubergen R.P. and Kolb J.A. (1962). High-resolution autoradiography. I. Methods. J. Cell Biol. 15, 173-188.

Conner G.E., Nelson D., Wisniewolski R., Lahita R.G., Blobel G. and Kunkel H.G. (1982). Protein antigens of the RNA-protein complexes detected by anti-SM and anti-RNP antibodies found in serum of patients with systemic lupus erythematosus and related disorders. J. Exp. Med. 156, 1475-1485.

Davis L., Banker G.A. and Steward O. (1987). Selective dendritic transport of RNA in hippocampal neurons in culture. Nature 330, 477-479.

Dix D.J. and Eisenberg B.R. (1990). Myosin mRNA accumulation and myofibrillogenesis at the myotendinous junction of stretched muscle fibers. J. Cell Biol. 111, 1885-1894.

Dvorak A.M. (1987). Monograph — Procedural guide to specimen handling for the ultrastructural pathology service laboratory. J. Electron Microsc. Tech. 6, 255-301.

Dvorak A.M. (1989). Human Mast Cells. Volume 14 in the series Advances in Anatomy, Embryology, and Cell Biology. Beck F., Hild W., Kriz W., Ortmann R., Pauly J.E. and Schiebler T.H. (eds.). Springler-Verlag. Berlin. pp 1-107.

Dvorak A.M. (1991). Basophil and mast cell degranulation and recovery. Volume 4 in the series Blood Cell Biochemistry. Harris J.R. (series, Dvorak A.M., vol. ed). Plenum Press. New York. pp 27-65.

Dvorak A.M. and Morgan E.S. (1998). Ribonuclease-gold labels heparin in human mast cell granules: New use for an ultrastructural enzyme affinity technique. J. Histochem. Cytochem. 46, 695-706.

Dvorak A.M. and Morgan E.S. (1999). Ribonuclease-gold ultrastructural localization of heparin in isolated human lung mast cells stimulated to undergo anaphylactic degranulation and recovery in vitro. Clin. Exp. Allergy 29, 1118-1128.

Dvorak A.M. and Morgan E.S. (2000a). Ultrastructural cytochemical, immunocytochemical and in situ hybridization methods with polyuridine probes detect mRNA in human mast cell granules. Histochem. J. 32, 423-438.

Dvorak A.M. and Morgan E.S. (2000b). Ultrastructural immunogold cytochemistry with autoimmune human sera and an antibody to uridine implicate human mast cell granules in RNA biology. Histochem. J. 32, 685-696.

Dvorak A.M. and Morgan E.S. (2001). Ribosomes and secretory granules in human mast cells: close associations demonstrated by staining with a chelating agent. Immunol. Rev. 179, 94-101.

Dvorak A.M. and Morgan E.S. (2002). The case for extending storage and secretion functions of human mast cell granules to include synthesis. In: Graumann W., Bendayan M., Bosman F T., Dvorak A M., Heitz PhU, Hirano H., Larsson L-I, Ramaeker F.C. and Schumacher U. (eds). Urban and Fischer. Jena, Germany. pp 229-320.

Dvorak A.M., Dvorak H.F., Peters S.P., Schulman E.S., MacGlashan D.W. Jr., Pyne K., Harvey V.S., Galli S.J. and Lichtenstein L.M. (1983). Lipid bodies: Cytoplasmic organelles important to arachidonate metabolism in macrophages and mast cells - [republished in J. Immunol. 132, 1586-1597, 1984]. J. Immunol. 131, 2965-2976.

Dvorak A.M., Hammel I., Schulman E.S., Peters S.P., MacGlashan D.W. Jr., Schleimer R.P., Newball H.H., Pyne K., Dvorak H.F., Lichtenstein L.M. and Galli S.J. (1984). Differences in the behavior of cytoplasmic granules and lipid bodies during human lung mast cell degranulation. J. Cell Biol. 99, 1678-1687.

Dvorak A.M., Schulman E.S., Peters S.P., MacGlashan D.W. Jr., Newball H.H., Schleimer R.P. and Lichtenstein L.M. (1985). Immunoglobulin E-mediated degranulation of isolated human lung mast cells. Lab. Invest. 53, 45-56.

Dvorak A.M., Schleimer R.P., Schulman E.S. and Lichtenstein L.M. (1986). Human mast cells use conservation and condensation mechanisms during recovery from degranulation. In vitro studies with mast cells purified from human lungs. Lab. Invest. 54, 663-678.

Dvorak A.M., Schleimer R.P. and Lichtenstein L.M. (1987). Morphologic mast cell cycles. Cell. Immunol. 105, 199-204.

Dvorak A.M., Schleimer R.P. and Lichtenstein L.M. (1988b). Human mast cells synthesize new granules during recovery from degranulation. In vitro studies with mast cells purified from human lungs. Blood 71, 76-85.

Dvorak A.M., Letourneau L., Login G.R., Weller P.F. and Ackerman S.J. (1988a). Ultrastructural localization of the Charcot-Leyden crystal protein (lysophospholipase) to a distinct crystalloid-free granule population in mature human eosinophils. Blood 72, 150-158.

Dvorak A.M., Morgan E.S., Lichtenstein L.M. and Schleimer R. (2000a). Ultrastructural autoradiographic analysis of RNA in isolated human lung mast cells during secretion and recovery from secretion. Int. Arch. Allergy Immunol. 122, 124-136.

Dvorak A.M., Morgan E.S., Lichtenstein L.M., Weller P.F. and Schleimer R.P. (2000b). RNA is closely associated with human mast cell secretory granules, suggesting a role(s) for granules in synthetic processes. J. Histochem. Cytochem. 48, 1-12.

Dvorak A.M., Morgan E.S. and Weller P.F. (2001). Ultrastructural immunolocalization of basic fibroblast growht factor to lipid bodies and secretory granules of human mast cells. Histochem. J. 33, 397-402.

Dworetzky S.I. and Feldherr C.M. (1988). Translocation of RNA-coated gold particles through the nuclear pores of oöcytes. J. Cell Biol. 106, 575-584.

Eliceiri G.L. and Gurney T. Jr. (1978). Subcellular location of precursors to small nuclear RNA species C and D and of newly synthesized 5S RNA in HeLa cells. Biochem. Biophys. Res. Commun. 81, 915-919.

Elkon K., Skelly S., Parnassa A., Moller W., Danho W., Weissbach H. and Brot N. (1986). Identification and chemical synthesis of a ribosomal protein antigenic determinant in systemic lupus erythematosus. Proc. Natl. Acad. Sci. USA 83, 7419-7423.

Elkon K.B. and Culhane L. (1984). Partial immunochemical characterization of the Ro and La proteins using antibodies from patients with the sicca syndrome and lupus erythematosus. J.

Immunol. 132, 2350-2356.

Elkon K.B., Parnassa A.P. and Foster C.L. (1985). Lupus autoantibodies target ribosomal P proteins. J. Exp. Med. 162, 459-471.

Etkin L.D. and Lipshitz H.D. (1999). RNA localization. FASEB J. 13, 419-420.

Fakan S. (1994). Perichromatin fibrils are in situ forms of nascent transcripts. Trends Cell Biol. 4, 86-90.

Fakan S. and Bernhard W. (1971). Localisation of rapidly and slowly labelled nuclear RNA as visualized by high resolution autoradiography. Exp. Cell Res. 67, 129-141.

Fakan S. and Bernhard W. (1973). Nuclear labelling after prolonged 3H-uridine incorporation as visualized by high resolution autoradiography. Exp. Cell Res. 79, 431-444.

Fakan S. and Puvion E. (1980). The ultrastructural visualization of nucleolar and extranucleolar RNA synthesis and distribution. Int. Rev. Cytol. 65, 255-299.

Fakan S., Puvion E. and Spohr G. (1976). Localization and characterization of newly synthesized nuclear RNA in isolated rat hepatocytes. Exp. Cell Res. 99, 155-164.

Farris A.D., Puvion-Dutilleul F., Puvion E., Harley J.B. and Lee L.A. (1997). The ultrastructural localization of 60-kDa Ro protein and human cytoplasmic RNAs: Association with novel electron-dense bodies. Proc. Natl. Acad. Sci. USA 94, 3040-3045.

Forster A.C., McInnes J.L., Skingle D.C. and Symons R.H. (1985). Non-radioactive hybridization probes prepared by the chemical labelling of DNA and RNA with a novel reagent, photobiotin. Nucleic Acids Res. 13, 745-761.

Franke W.W., Hergt M. and Grund C. (1987). Rearrangement of the vimentin cytoskeleton during adipose conversion: formation of an intermediate filament cage around lipid globules. Cell 49, 131-141.

Frens G. (1973). Controlled nucleation for the regulation of the particle size in monodisperse gold suspensions. Nature Physic. Sci. 241, 20-22.

Fulton A.B., Wan K.M. and Penman S. (1980). The spatial distribution of polyribosomes in 3T3 cells and the associated assembly of proteins into the skeletal framework. Cell 20, 849-857.

Galli S.J., Dvorak A.M., Peters S.P., Schulman E.S., MacGlashan D.W., Jr., Isomura T., Pyne K., Harvey V.S., Hammel I., Lichtenstein L.M. and Dvorak H.F. (1985). Lipid bodies — Widely distributed cytoplasmic structures that represent preferential nonmembrane repositories of exogenous [^{3}H]arachidonic acid incorporated by mast cells, macrophages, and other cell types. In: J.M. Bailey. (ed.). Plenum Press. New York. pp. 221-239.

Garner C.C., Tucker R.P. and Matus A. (1988). Selective localization of messenger RNA for cytoskeletal protein MAP2 in dendrites. Nature 336, 674-677.

Geoghegan W.D. and Ackerman G.A. (1977). Adsorption of horseradish peroxidase, ovomucoid and anti-immunoglobulin to colloidal gold for the indirect detection of concanavalin A, wheat germ agglutinin and goat anti-human immunoglobulin G on cell surfaces at the electron microscopic level: A new method, theory and application. J. Histochem. Cytochem. 25, 1187-1200.

Gordon J.R., Burd P.R. and Galli S.J. (1990). Mast cells as a source of multifunctional cytokines. Immunol. Today 11, 458-464.

Gottlieb E. (1990). Messenger RNA transport and localization. Curr. Opin. Cell Biol. 2, 1080-1086.

Gray M.W. and Cedergren R. (1993). The new age of RNA. FASEB J. 7, 4-6.

Hammel I., Dvorak A.M., Peters S.P., Schulman E.S., Dvorak H.F., Lichtenstein L.M. and Galli S.J. (1985). Differences in the volume distributions of human lung mast cell granules and lipid bodies: Evidence that the size of these organelles is regulated by distinct mechanisms. J. Cell Biol. 100, 1488-1492.

Hardin J.A., Rahn D.R., Shen C., Lerner M.R., Wolin S.L., Rosa M.D. and Steitz J.A. (1982). Antibodies from patients with connective tissue diseases bind specific subsets of cellular RNA-protein particles. J. Clin. Invest. 70, 141-147.

Hazelrigg T. (1998). The destinies and destinations of RNAs. Cell 95, 451-460.

Heinrichs V., Bach M., Winkelmann G. and Lührmann R. (1990). U1-specific protein C needed for efficient complex formation of U1 snRNP with a 5´ splice site. Science 247, 69-72.

Hendrick J.P., Wolin S.L., Rinke J., Lerner M.R. and Steitz J.A. (1981). Ro small cytoplasmic ribonucleoproteins are a subclass of La ribonucleoproteins: Further characterization of the Ro and La small ribonucleoproteins from uninfected mammalian cells. Mol. Cell. Biol. 1, 1138-1149.

Hill M.A., Schedlich L. and Gunning P. (1994). Serum-induced signal transduction determines the peripheral location of ß-actin mRNA within the cell. J. Cell Biol. 126, 1221-1230.

Hinterberger M., Pettersson I. and Steitz J.A. (1983). Isolation of small nuclear ribonucleoproteins containing U1, U2, U4, U5, and U6 RNAs. J. Biol. Chem. 258, 2604-2613.

Hiriyanna K.T., Varkey J., Beer M. and Benbow R.M. (1988). Electron microscopic visualization of sites of nascent DNA synthesis by streptavidin-gold binding to biotinylated nucleotides incorporated in vivo. J. Cell Biol. 107, 33-44.

Horisberger M. and Rosset J. (1977). Colloidal gold, a useful marker for transmission and scanning electron microscopy. J. Histochem. Cytochem. 25, 295-305.

Isaacs W.B. and Fulton A.B. (1987). Cotranslational assembly of myosin heavy chain in developing cultured skeletal muscle. Proc. Natl. Acad. Sci. USA 84, 6174-6178.

Jansen R.-P. (1999). RNA-cytoskeletal associations. FASEB J. 13, 455-466.

Jirikowski G.F., Sanna P.P. and Bloom F.E. (1990). mRNA coding for oxytocin is present in axons of the hypothalamo-neurohypophysial tract. Proc. Natl. Acad. Sci. USA 87, 7400-7404.

Jirikowski G.F., Sanna P.P., Maciejewski-Lenoir D. and Bloom F.E. (1992). Reversal of diabetes insipidus in Brattleboro rats: Intrahypothalamic injection of vasopressin mRNA. Science 255, 996-998.

Kislauskis E.H., Zhu X. and Singer R.H. (1994). Sequences responsible for intracellular localization of b-actin messenger RNA also affect cell phenotype. J. Cell Biol. 127, 441-451.

Knowles R.B., Sabry J.H., Martone M.E., Deerinck T.J., Ellisman M.H., Bassell G.J. and Kosik K.S. (1996). Translocation of RNA granules in living neurons. J. Neurosci. 16, 7812-7820.

Kobayasi T., Midtgård K. and Asboe-Hansen G. (1968). Ultrastructure of human mast-cell granules. J. Ultrastruct. Res. 23, 153-165.

Konarska M.M. and Sharp P.A. (1987). Interactions between small nuclear ribonucleoprotein particles in formation of spliceosomes. Cell 49, 763-774.

Kopriwa B.M. (1973). A reliable, standardized method for ultrastructural electron microscopic radioautography. Histochemie 37, 1-17.

Kopriwa B. (1975). A comparison of various procedures for fine grain development in electron microscopic radioautography. Histochemistry 44, 201-224.

Kopriwa B.M., Levine G.M. and Nadler N.J. (1984). Assessment of resolution by half distance values for tritium and radioiodine in electron microscopic radioautographs using Ilford L4 emulsion developed by "solution physical" or D-19b methods. Histochemistry 80, 519-522.

Krämer A., Keller W., Appel B. and Luhrmann R. (1984). The 5' terminus of the RNA moiety of U1 small nuclear ribonucleoprotein particles is required for the splicing of messenger RNA precursors. Cell 38, 299-307.

Kuo H.-C., Nasim F.-U.H. and Grabowski P.J. (1991). Control of alternative splicing by the differential binding of U1 small nuclear ribonucleoprotein particle. Science 251, 1045-1050.

Laitala-Leinonen T., Howell M.L., Dean G.E. and Väänänen H.K. (1996). Resorption-cycle-dependent polarization of mRNAs for different subunits of V-ATPase in bone-resorbing osteoclasts. Mol. Biol. Cell 7, 129-142.

Lamb M.M. and Laird C.D. (1976). Increase in nuclear poly(A)-containing RNA at syncytial blastoderm in Drosophila melanogaster embryos. Dev. Biol. 52, 31-42.

Langer P.R., Waldrop A.A. and Ward D.C. (1981). Enzymatic synthesis of biotin-labeled polynucleotides: Novel nucleic acid affinity probes. Proc. Natl. Acad. Sci. USA 78, 6633-6637.

Lasko P. (1999). RNA sorting in Drosophila oocytes and embryos. FASEB J. 13, 421-433.

Lenk R., Ransom L., Kaufmann Y. and Penman S. (1977). A cytoskeletal structure with associated polyribosomes obtained from HeLa cells. Cell 10, 67-78.

Lindahl U. and Höök M. (1978). Glycosaminoglycans and their binding to biological macromolecules. Annu. Rev. Biochem. 47, 385-417.

Lobo S.M. and Hernandez N. (1989). A 7 bp mutation converts a human RNA polymerase II snRNA promoter into an RNA polymerase III promoter. Cell 58, 55-67.

Madore S.J., Wieben E.D. and Pederson T. (1984). Intracellular site of U1 small nuclear RNA processing and ribonucleoprotein assembly. J. Cell Biol. 98, 188-192.

Maniatis T. and Reed R. (1987). The role of small nuclear ribonucleoprotein particles in pre-mRNA splicing. Nature 325, 673-678.

Martone M.E., Pollock J.A., Jones Y.Z. and Ellisman M.H. (1996). Ultrastructural localization of dendritic messenger RNA in adult rat hippocampus. J. Neurosci. 16, 7437-7446.

Mattaj I.W. (1990). Splicing stories and poly(A) tales: an update on RNA processing and transport. Curr. Opin. Cell Biol. 2, 528-538.

McInnes J.L., Dalton S., Vize P.D. and Robins A.J. (1987). Nonradioactive photobiotin-labeled probes detect single copy genes and low abundance mRNA. Biotechnology 5, 269-272.

McNeilage L.J., Whittingham S., Jack I. and Mackay I.R. (1985). Molecular analysis of the RNA and protein components recognized by anti-La(SS-B) autoantibodies. Clin. Exp. Immunol. 62, 685-695.

Mehlin H., Daneholt B. and Skoglund U. (1992). Translocation of a specific premessenger ribonucleoprotein particle through the nuclear pore studied with electron microscope tomography. Cell 69, 605-613.

Merlie J.P. and Sanes J.R. (1985). Concentration of acetylcholine receptor mRNA in synaptic regions of adult muscle fibres. Nature 317, 66-68.

Metcalfe D.D., Kaliner M. and Donlon M.A. (1981). The mast cell. CRC Crit. Rev. Immunol. 3, 23-74.

Mount S.M., Pettersson I., Hinterberger M., Karmas A. and Steitz J.A. (1983). The U1 small nuclear RNA-protein complex selectively binds a 5´ splice site in vitro. Cell 33, 509-518.

Mowry K.L. and Cote C.A. (1999). RNA sorting in *Xenopus* oocytes and embryos. FASEB J. 13, 435-445.

Murphy D.J. (2001). The biogenesis and functions of lipid bodies in animals, plants and microorganisms. Prog. Lipid Res. 40, 325-438.

Oleynikov Y. and Singer R.H. (1998). RNA localization: Different zipcodes, same postman? Trends Cell Biol. 8, 381-383.

Ornelles D.A., Fey E.G. and Penman S. (1986). Cytochalasin releases mRNA from the cytoskeletal framework and inhibits protein synthesis. Mol. Cell. Biol. 6, 1650-1662.

Padgett R.A., Mount S.M., Steitz J.A. and Sharp P.A. (1983). Splicing of messenger RNA precursors is inhibited by antisera to small nuclear ribonucleoprotein. Cell 35, 101-107.

Palade G.E. (1955). A small particulate component of the cytoplasm. J. Biophys. Biophys. Biochem. Cytol. 1, 59-68.

Palade G.E. and Porter K.R. (1954). Studies on the endoplasmic reticulum. I. Its identification in cells in situ. J. Exp. Med. 100, 641-662.

Palade G.E. and Siekevitz P. (1956a). Liver microsomes. An integrated morphological and biochemical study. J. Biophys. Biochem. Cytol. 2, 171-200.

Palade G.E. and Siekevitz P. (1956b). Pancreatic microsomes. An integrated morphological and biochemical study. J. Biophys. Biochem. Cytol. 2, 671-690.

Patton J.G. and Wieben E.D. (1987). U1 precursors: Variant 3´ flanking sequences are transcribed in human cells. J. Cell Biol. 104, 175-182.

Perry R.P. (1981). RNA processing comes of age. J. Cell Biol. 91, 28s-38s.

Pettersson I., Hinterberger M., Mimori T., Gottlieb E. and Steitz J.A. (1984). The structure of mammalian small nuclear ribonucleoproteins. Identification of multiple protein components reactive with anti-(U1)ribonucleoprotein and anti-Sm autoantibodies. J. Biol. Chem. 259, 5907-5914.

Qu Z., Huang X., Ahmadi P., Stenberg P., Liebler J.M., Le A.-C., Planck S.R. and Rosenbaum J.T. (1998a). Synthesis of basic fibroblast growth factor by murine mast cells. Regulation by transforming growth factor beta, tumor necrosis factor-alpha, and stem cell factor. Int. Arch. Allergy Immunol. 115, 47-54.

Qu Z., Kayton R.J., Ahmadi P., Liebler J.M., Powers M.R., Planck S.R. and Rosenbaum J.T. (1998b). Ultrastructural immunolocalization of basic fibroblast growth factor in mast cell secretory granules: Morphological evidence for bFGF release through degranulation. J. Histochem. Cytochem. 46, 1119-1128.

Reddy R. and Busch H. (1983). Small nuclear RNAs and RNA processing. Prog. Nucleic Acid Res. Mol. Biol. 30, 127-162.

Reed R., Griffith J. and Maniatis T. (1988). Purification and visualization of native spliceosomes. Cell 53, 949-961.

Reynolds E.S. (1963). The use of lead citrate at high pH as an electron-opaque stain in electron microscopy. J. Cell Biol. 17, 208-212.

Rings E.H.H.M., Büller H., A.Neele A.M. and Dekker J. (1994). Protein sorting versus messenger RNA sorting? Eur. J. Cell Biol. 63, 161-171.

Rinke J. and Steitz J.A. (1982). Precursor molecules of both human 5S ribosomal RNA and transfer RNAs are bound by a cellular protein reactive with anti-La lupus antibodies. Cell 29, 149-159.

Ruby S.W. and Abelson J. (1988). An early hierarchic role of U1 small nuclear ribonucleoprotein in spliceosome assembly. Science 242,

1028-1035.

Salmivirta M., Lidholt K. and Lindahl U. (1996). Heparan sulfate: A piece of information. FASEB J. 10, 1270-1279.

Schulman E.S., MacGlashan D.W. Jr., Peters S.P., Schleimer R.P., Newball H.H. and Lichtenstein L.M. (1982). Human lung mast cells: Purification and characterization. J. Immunol. 129, 2662-2667.

Schur P.H., Moroz L.A. and Kunkel H.G. (1967). Precipitating antibodies to ribosomes in the serum of patients with systemic lupus erythematosus. Immunochemistry 4, 447-453.

Schwartz L.B. and Austen K.F. (1984). Structure and function of the chemical mediators of mast cells. In: K. Ishizaka (ed.). S. Karger. Basel. pp 271-321.

Simons F.H.M., Pruijn G.J.M. and van Venrooij W.J. (1994). Analysis of the intracellular localization and assembly of Ro ribonucleoprotein particles by microinjection into Xenopus laevis oocytes. J. Cell Biol. 125, 981-988.

Singer R.H. (1992). The cytoskeleton and mRNA localization. Curr. Opin. Cell Biol. 4, 15-19.

Singer R.H. (1993). RNA zipcodes for cytoplasmic addresses. Intracellular localization of mRNAs appears to be determined by sequences in their 3 untranslated regions that are composed of multiple elements. Curr. Biol. 3, 719-721.

Singer R.H. and Ward D.C. (1982). Actin gene expression visualized in chicken muscle tissue culture by using in situ hybridization with a biotinated nucleotide analog. Proc. Natl. Acad. Sci. USA 79, 7331-7335.

Sobel S.G. and Wolin S.L. (1999). Two yeast La motif-containing proteins are RNA binding proteins that associate with polyribosomes. Mol. Biol. Cell 10, 3849-3862.

St. Clair E.W. (1992). Anti-La antibodies. Rheu. Dis. Clin. of North Am. 18, 359-376.

St. Johnston D. (1995). The intracellular localization of messenger RNAs. Cell 81, 161-170.

Steiner G., Skriner K. and Smolen J.S. (1996). Autoantibodies to the A/B proteins of the heterogeneous nuclear ribonucleoprotein complex: Novel tools for the diagnosis of rheumatic diseases. Int. Arch. Allergy Immunol. 111, 314-319.

Stevens R.L., Fox C.C., Lichtenstein L.M. and Austen K.F. (1988). Identification of chondroitin sulfate E proteoglycans and heparin proteoglycans in the secretory granules of human lung mast cells. Proc. Natl. Acad. Sci. USA 85, 2284-2287.

Steward O. and Levy W.B. (1982). Preferential localization of polyribosomes under the base of dendritic spines in granule cells of the dentate gyrus. J. Neurosci. 2, 284-291.

Tan E.M. (1991). Autoantibodies in pathology and cell biology. Cell 67, 841-842.

Thompson H.L., Schulman E.S. and Metcalfe D.D. (1988). Identification of chondroitin sulfate E in human lung mast cells. J. Immunol. 140, 2708-2713.

Weller P.F. and Dvorak A.M. (1985). Arachidonic acid incorporation by cytoplasmic lipid bodies of human eosinophils. Blood 65, 1269-1274.

Weller P.F., Ackerman S.J., Nicholson-Weller A. and Dvorak A.M. (1989). Cytoplasmic lipid bodies of human neutrophilic leukocytes. Am. J. Pathol. 135, 947-959.

Weller P.F., Monahan-Earley R.A., Dvorak H.F. and Dvorak A.M. (1991a). Cytoplasmic lipid bodies of human eosinophils. Subcellular isolation and analysis of arachidonate incorporation. Am. J. Pathol. 138, 141-148.

Weller P.F., Ryeom S.W. and Dvorak A.M. (1991b). Lipid bodies: Structurally distinct, nonmembranous intracellular sites of eicosanoid formation. In: Bailey J.M. (ed.). Plenum Press. New York. pp 353-362.

Weller P.F., Ryeom S.W., Picard S.T., Ackerman S.J. and Dvorak A.M. (1991c). Cytoplasmic lipid bodies of neutrophils: Formation induced by cis-unsaturated fatty acids and mediated by protein kinase C. J. Cell Biol. 113, 137-146.

White P.J. and Hoch S.O. (1981). Definition of the antigenic polypeptides in the Sm and RNP ribonucleoprotein complexes. Biochem. Biophys. Res. Commun. 102, 365-371.

Wilhelm J.E. and Vale R.D. (1993). RNA on the move: The mRNA localization pathway. J. Cell Biol. 123, 269-274.

Wolin S.L. and Steitz J.A. (1984). The Ro small cytoplasmic ribonucleoproteins: Identification of the antigenic protein and its binding site on the Ro RNAs. Proc. Natl. Acad. Sci. USA 81, 1996-2000.

Yoo C.J. and Wolin S.L. (1997). The yeast La protein is required for the 3´endonucleolytic cleavage that matures tRNA precursors. Cell 89, 393-402.

Zweytick D., Athenstaedt K. and Daum G. (2000). Intracellular lipid particles of eukaryotic cells. Biochim. Biophys. Acta1469, 101-120.

Accepted February 24, 2002